Journal of Materials Science: Materials in Electronics

Effects of carbon nanotubes on the AC conductivity, permittivity, and electromagnetic shielding performance of polyurethane foams in the 15 Hz – 26.5 GHz frequency range

--Manuscript Draft--

Manuscript Number:	JMSE-D-25-03626R1
Full Title:	Effects of carbon nanotubes on the AC conductivity, permittivity, and electromagnetic shielding performance of polyurethane foams in the 15 Hz – 26.5 GHz frequency range
Article Type:	Original Research
Keywords:	carbon nanotubes; polyurethane; permittivity; numerical simulation; shielding effectiveness; microwave Absorption
Corresponding Author:	Ahmad Mamoun KHAMIS Catholic University of Louvain: Universite Catholique de Louvain Ottignies-Louvain-la-Neuve, BELGIUM
Corresponding Author Secondary Information:	
Corresponding Author's Institution:	Catholic University of Louvain: Universite Catholique de Louvain
Corresponding Author's Secondary Institution:	
First Author:	Ahmad Mamoun KHAMIS
First Author Secondary Information:	
Order of Authors:	Ahmad Mamoun KHAMIS
	Laetitia Urbanczyk
	Christophe Detrembleur
	Isabelle Huynen
Order of Authors Secondary Information:	
Funding Information:	FEDER — Prof. Isabelle Huynen
Abstract:	This study investigates the impact of increasing carbon nanotube (CNT) concentration on the AC conductivity, dielectric, and electromagnetic shielding properties of polyurethane (PU) foams. Four CNT-PU foam samples with different CNT contents (1 wt.%, 2.3 wt.%, 6 wt.%, and 11.2 wt.%) were fabricated using the dip coating method. Three different measurement techniques were employed to characterize the AC conductivity and complex permittivity of the CNT-PU composites across various frequency ranges (kHz, MHz, and GHz). COMSOL software was also used to calculate the scattering parameters and visualise the electric field distribution. The microstructure SEM images of CNT-PU samples confirmed that the CNTs formed interconnected and well-distributed networks on the PU surface skeleton, leading to conductive pathways that boost the absorption loss. Therefore, increasing CNT content increased the permittivity and conductivity of CNT-PU samples, and consequently, the total shielding effectiveness (SET). The incorporation of 11.2 wt.% CNT greatly enhanced the AC conductivity, increasing it from 3.6 × 10-6 S/cm (pure PU) to 0.0068 S/cm at 10 MHz. Furthermore, the corresponding values of complex permittivity also increased from 1.32 – j 0.0059 to 8.65 – j 3.7 at 1000 MHz. The complex permittivity of 11.2 wt.% CNT sample was 3.76 – j 3.56 at 25 GHz. The samples with 6 wt.% CNT and 11.2 wt.% CNT met the standard requirements for the electromagnetic interference shielding applications because their total shielding effectiveness (SET) values surpassed the 20 dB threshold within the 18 – 26.5 GHz frequency range. The visualization of the electric field distribution further confirmed that the 11.2 wt.% CNT sample greatly attenuated the electric field propagation through the material. The contribution of the absorption loss mechanism to the SET of CNT-PU samples surpassed 94% in the 18 – 26.5 GHz frequency range, indicating that the absorption loss was the main shielding mechanism in our samples.

Additional Information:	
Question	**Response**
Journal of Materials Science: Materials in Electronics considers only outstanding papers that make a distinct contribution to the field of experimental electronic materials. This includes optoelectronic and photonic materials as well. Please explain in point form why your work is outstanding and what distinguishes this work from past work. What are the outstanding and exceptional contributions of this paper? How does it contribute to the state-of-the art?	A dielectric material test set using a parallel plate capacitive configuration is used for the first time to measure the permittivity of composite conductive foams. Our work fills a gap in the literature by proposing a solution for non-destructive characterization of foams over a wide frequency range. The combination of SEM imagery, frequency measurements, and COMSOL simulations provides a comprehensive analysis that aids in the design of composite foams for electromagnetic shielding applications
Is this manuscript part of an ongoing Special Issue (SI), and were you asked to submit to this Special Issue?	No
Were you asked by one of our editors to resubmit your manuscript because of textual overlap or not complying with scientific guidelines?	No
Does your manuscript comply with the journal's standards and instructions to authors on notation, significant figures, experimental errors and the use of the Scherrer equation? Instructions to authors can be accessed at "https://www.springer.com/journal/10854/submission-guidelines#linksAndDownloads". Manuscripts that do not comply with instructions to authors will be rejected.	Yes
How many of your own papers have you self-cited in this manuscript? (Your paper may be rejected if the Editor feels self-citations are excessive or not related to the work in the paper)	1

UCLouvain
Institute of Information and
Communication Technologies, Electronics
and Applied Mathematics (ICTEAM)

icteam

Prof. Dr. Furong Zhu
Editor of Journal of Materials
Science: Materials in Electronics

September 8, 2025

Dear Editor,

We are pleased to submit the revised version of our manuscript, JMSE-D-25-03626. We greatly appreciate the opportunity to improve it based on the editors' and reviewers' comments.

The comments of the reviewers were accordingly and carefully addressed, and all changes were highlighted in yellow. The manuscript was also enriched with new relevant studies.

We hope that the reviewers and editors will evaluate positively the revised manuscript for publication in the Journal of Materials Science: Materials in Electronics. Our responses to the valuable comments of the reviewers and editors are attached to this letter.

We are looking forward to receiving your feedback.

Sincerely yours,

Dr. Ahmad KHAMIS,
Corresponding author

LOUVAIN-LA-NEUVE | BRUXELLES | MONS | TOURNAI | CHARLEROI | NAMUR
Place du Levant, 3 - PO Box L5.03.02 - 1348 Louvain-la-Neuve, Belgium
Tél. +32 (0)10 47 23 08 – fax +32 (0)10 47 21 80 – ahmad.khamis@uclouvain.be – www.uclouvain.be/icteam

Revision of manuscript JMSE-D-25-03626

Answers to the comments of the Editor

We thank the Editor for reviewing our manuscript and making valuable comments. We have carefully addressed each comment by the Editor and reviewers below.
Changes made in response to comments are highlighted in yellow in the revised manuscript.

Comment 1:
Please modify your manuscript as appropriate and provide replies to the referee comments. Please identify the revisions in the new manuscript by highlighting them in yellow.

Answer to comment 1:
The manuscript has been modified and improved as appropriate. The reviewer comments were carefully addressed. The revisions in the revised manuscript have been highlighted in yellow.

Comment 2:
If you are citing references from this journal that have been published in the last 3 years, please ensure that the references are relevant. We would like to eliminate unnecessary self-citations of the journal itself.

Answer to comment 2:
The references used in our manuscript are relevant.

Comment 3:
If the referees have suggested the inclusion of certain references, please ensure that these are relevant to the work and explain to the editor why they are or are not relevant in your reply letter.

Answer to comment 3:
The referees did not suggest including certain references.

Comment 4:
VERY IMPORTANT: You must follow the author instructions in the online document "JMSE Guidelines for Authors on Notation and Best Scientific Practice" at https://eur03.safelinks.protection.outlook.com/?url=https%3A%2F%2Fwww.springer.com%2Fjournal%2F10854%2Fsubmission-guidelines%23linksAndDownloads&data=05%7C02%7Cahmad.khamis%40uclouvain.be%7C04a3599a3b0f441c79f408ddd8c09477%7C7ab090d4fa2e4ecfbc7c4127b4d582ec%7C1%7C0%7C638905043819476864%7CUnknown%7CTWFpbGZsb3d8eyJFbXB0eU1hcGkiOnRydWUsIlYiOiIwLjAuMDAwMCIsIlAiOiJXaW4zMiIsIkFOIjoiTWFpbCIsIldUIjoyfQ%3D%3D%7C0%7C%7C%7C&sdata=f7qcpC%2Bs7fHSRUNcATcXm7PkZlh2TctyZxe5wrjXMUE%3D&reserved=0

Answer to comment 4:
We have read and followed the instructions of this online document.

Comment 5:
VERY IMPORTANT: Your manuscript must comply with the journal's requirements on notation (including the use of points for decimals and not commas), the use of significant figures, errors and uncertainties, the use of the Scherrer equation, Williamson-Hall analysis and the depiction of smooth curves through the experimental points. Manuscripts that do not comply with JMSE's requirements will be rejected.

Answer to comment 5:
We followed the mentioned requirements in our manuscript.

Comment 6:
The title of your paper must represent the work without superlative adjectives and without unjustifiable claims such as "amazing", "extraordinary", "unbelievable", "outstanding" etc. If necessary, please modify the title of your paper. (See link under Point (4) above.)

Answer to comment 6:

The title of our manuscript does not contain such unjustifiable claims.

Answers to the comments of Reviewer 2

We thank the reviewer for the valuable comments on our manuscript. Such comments enhance the quality and clarity of our work.
The manuscript was carefully modified to address all comments, and the changes were highlighted in yellow in the revised manuscript.

Comment 1:
Clearly emphasize why your study on CNT-PU foams and their dielectric properties over such a broad frequency range is important compared to prior work.

Answer to comment 1:
The broad frequency range can increase the number of applications where the samples may be implemented.
The following two sentences were added to the introduction:
"It is important to note that the number of EM applications (such as EMI shielding) in which a certain material can be used depends on its EM properties at specific frequency ranges. Therefore, investigating the EM properties over a broad frequency range will increase the number of applications where the material may be used, compared to a narrow frequency range"
"Several applications are covered in these frequency ranges including marine communications in the 30 - 300 kHz range, television, microwave, and mobile phones in the 300 MHz – 1 GHz range, and satellite communications in the 10 – 26.5 GHz range."

Comment 2:
Highlight any unique aspects of your sample preparation or characterization (e.g., the 3D holder for DMTF) and why these overcome limitations in the field.

Answer to comment 2:
We have highlighted in section 2.2 the unique aspect of our sample preparation as follows:
"In this study, the dip coating method is chosen for the fabrication of CNT-PU foam samples because of three advantages: it is the most cost-effective, the fabricated foam can be used directly without post-processing, and finally the foam is fully covered with the applied nanofiller."

The importance of using the 3D holder for DMTF was highlighted in the introduction. The following sentences were added "Such pressing decreases the thickness of the foam sample under test, leading to the following problems: the content of air inside the foam sample will decrease, which may result in wrong values of dielectric constant; it is not possible to measure the new thickness of the foam sample after the upper electrode presses the foam sample, and finally it is not possible to obtain the real dielectric constant of the MUT since a significant change in dimensions occurred. ….. which will overcome the limitations of characterizing foam samples using DMTF."

Comment 3:
When presenting results (e.g., conductivity, permittivity, shielding effectiveness), compare them explicitly to prior literature values or benchmarks.

Answer to comment 3:
The following statements were added to compare our work with the literature:

In Section 4.2

"These results are consistent with a study conducted by Hoang [40]. Ilya also reported that the AC conductivity of PU is approximately 10^{-6} S/cm within the 10^5-10^6 frequency range [41]."

In section 4.3:
"The ε' values of PU sample reported in this study are in accordance with the ones reported by Wang [36]."

In addition, we added Table 2 in Section 4.5, in which we compared the SE_T values obtained in our study with the ones previously reported in the literature.

Comment 4:
Discuss how your results meet or exceed commercial standards (you mention 20 dB shielding effectiveness at 24.5 GHz) and what that implies practically.

Answer to comment 4:
In order to address this important comment, we added the following sentences in section 4.5 before Figure 9**:** "The good EMI shielding material causes a maximum attenuation of the EM wave by absorption or reflection with inappreciable transmission. When the SE_T of a certain material is 20 dB, this means that there is an attenuation of 99% of the total energy of the incident wave [54]. The EMI shielding requirements depend on the application. For example, the EMI shielding of 15-20 dB is considered an adequate level of shielding for desktop computers and laptops [55]."

Comment 5:
Quantify the improvement from CNT concentration increases more clearly.

Answer to comment 5:
Quantitative discussions were added to address this important comment. The following sentences were added to the manuscript:

In section 4.2 before equation 1:
"At 10 MHz, the σ_{ac} values were 0.00048 S/cm, 0.0012 S/cm, 0.0037 S/cm, and 0.0068 S/cm for the 1 wt.% CNT, 2.3 wt.%, 6 wt.%, and 11.2 wt.% samples, respectively. This indicates that the σ_{ac} increased by 150%, 208%, and 83% by increasing the CNT concentration from 1 wt.% to 2.3%, 2.3 wt.% to 6 wt.%, and 6 wt.% to 11.2 wt.%, respectively"

In section 4.4, 2 paragraphs before Figure 8:
At 25 GHz, the ε' values were 1.37, 1.86, 2.39, and 3.76 for the 1 wt.%, 2.3 wt.%, 6 wt.%, and 11.2 wt.% CNT samples while the corresponding values of ε'' were 0.44, 0.82, 2.07, and 3.56. This indicates that the ε' and ε'' increased by 36% and 86% with increasing the CNT concentration from 1 wt.% to 2.3 wt.%. "

In addition, Table 1 was added to present the values of complex permittivity of CNT-PU samples obtained using the impedance analyzer at 1000 MHz.

Comment 6:
Beyond EMI shielding, briefly discuss other possible applications for CNT-PU composites, such as sensors, flexible electronics, or thermal insulation.

Answer to comment 6:
Some applications of CNT-PU samples were added to the introduction as follows:
"The conductive PU composites can also be found in other applications such as environmental and medical sensing, electrochemical energy storage, and tissue regeneration [22]. Additionally, the CNT-PU nanocomposites have been studied in various fields such as bone substitute, cardiovascular applications, ligament, tendon, and neural tissue engineering [23]**.**

Comment 7:
Consider adding more details on sample reproducibility, error analysis, and measurement uncertainties.

Answer to comment 7:
The following was added to address the uncertainty topic:

In Section 3.1 before Figure 1:
"The uncertainty in the sample geometry was provided by manufacturer as follows: for a sample with a thickness of 0.1 mm, the error in the thickness has to be less than 1 µm for a 1% accurate result."

In section 3.1 before Figure 2:
"Measurement accuracy of impedance analyzer applies when the calibration is performed at 23 °C ± 5 °C. When the calibration is below 18 °C or above 28 °C, the measurement error doubles. The basic accuracy is ±0.65% and the impedance range is 120 mΩ to 52 kΩ (10% measurement accuracy range)."

In section 3.1 after Figure 1:
"The typical power level accuracy (dB) of the VNA is ± 0.60 for the 10 – 18 GHz frequency range."

Comment 8:
Can be consider to cite some similar references in introduction section.

Answer to comment 8:
The Introduction Section was improved, and eight new references were added.

Answers to the comments of Reviewer 3

We appreciate the constructive comments of the reviewer, which helped us improve the quality and readability of our manuscript. The comments were carefully and accordingly considered in the revised version of the manuscript, and all changes were highlighted in yellow.

Comment 1:
The authors may add graphical abstracts and highlights to make the manuscript easier to read.

Answer to comment 1:
After careful check of the guidelines of the journal, graphical abstract and highlights are not asked/mandatory.

Comment 2:
Improving the title is recommended; the title should be reflective and specific, and the primary methods and findings used in the study should be made clear and more focused. This title is more suitable for a review rather than a research paper.

Answer to comment 2:
The title has been modified into:
Effects of carbon nanotubes on the AC conductivity, permittivity, and electromagnetic shielding performance of polyurethane foams in the 15 Hz - 25 GHz frequency range

---

Comment 3:
The experimental synthesis protocol section should include a reference; otherwise, the authors should optimize the process under different parameters and conditions. Additionally, I recommend improving the material section on page 2, name and explain the brand of the materials you have used. Also, stop counting the techniques in the characterization section; explain them with a related title. The COMSOL simulation section should be described in detail, with associated citations and computational models description.

Answer to comment 3:
Two references were added to the Fabrication Section 2.2.
All the brands and names of the materials are mentioned in the paper. As these are commercial samples, their exact composition is not available.
The techniques counting was stopped, and the related titles were modified. The COMSOL Simulation (subsection 3.2) was improved.

Comment 4:
I strongly recommend improving the captions of all figures by providing detailed information and including labels.

Answer to comment 4:
The captions of all figures were improved as recommended.

Answers to the comments of Reviewer 4

We are thankful to the reviewer for his important and valuable comments on our manuscript. All comments were carefully addressed, and the changes were highlighted in yellow in the revised manuscript.

Comment 1:
Abstract must be enriched via valuable results which pave the way for understanding the audiences.

Answer to comment 1:
The abstract was enhanced based on the reviewer's comment.

Comment 2:
The novelty of this study should be inserted in the text clearly.

Answer to comment 2:
The novelty of this study has been clearly inserted in the text. Please, see our answer to comment 4 by the reviewer.

Comment 3:
The discussion section is very short compared to the obtained results. Please go through it and add more comments and interpretations.

Answer to comment 3:
In Section 3 "Results and Discussion" of the revised manuscript, results are carefully discussed taking into account the comments made by all reviewers.

Comment 4:
Please clearly mention the novelty of this work in the main parts of the article (introduction, method, results, and conclusion section).

Answer to comment 4:
The novelty of this work was clearly mentioned in various parts of the manuscript, for example at the end of the introduction, in Section 3 before subsection 3.1, as concerning the use of Comsol, and in Section 3.1, two paragraphs before Figure 2, concerning the 3D holder. Please, see also our answer to Comment 11 below.

Comment 5:
There are more and more errors in the standard of English (and other typo errors/mistakes), and then the authors should be proofread the paper carefully.

Answer to comment 5:
A proofreading was conducted for the manuscript.

Comment 6:
The introduction section is very short and poorly described. It doesn't present the reference to the manuscript scope. In the introduction section, authors should make an in-depth literature review concerning the application of advanced technologies such as nanotechnology and advanced crystalline materials and composites, and nanostructures for improving people's lives, environmental remediation, sensors, wastewater treatment, renewable and clean energy production and storage, addressing environmental issues, and optical applications. Introduction has deficiency citation to valuable works published before.

Answer to comment 6:
The introduction was improved according to the comments made by all reviewers.

Comment 7:
And the structure of the manuscript might need a major adjusting for a better understanding.

Answer to comment 7:
The manuscript was modified in some places for better readability and understanding.

Comment 8:
Redesign the chapter of proposed model the way so anybody can repeat your procedures.

Answer to comment 8:
Section 3.2 now includes all details enabling reproduction of the results from Comsol simulations.

Comment 9:
Results and discussion: - To increase the scientific value of the manuscript Authors should consider extension of the all results section with comparison of the obtained results with the results described in previous publications.

Answer to comment 9:
Our SE_T results were compared with previously published studies in Table 2.
Other comparisons with the values of the literature are provided as an answer to Comment 3 by Reviewer 2.

Comment 10:
Indeed, there are impressive amount of results. However, the conclusions section needs to improve with selected and highlighted main findings.

Answer to comment 10:
The conclusion was improved by highlighting the main findings.

Comment 11:
What is the main significance of paper in comparison to other published works?

Answer to comment 11:

Our work has several advantages compared to previously published works, such as:

1. Characterising our sample over a wide range of frequencies (kHz, MHz, and GHz).
2. Using the DMTF to characterise foamed samples for the first time.
3. Reporting EMI shielding materials, based on absorption mechanisms, with higher shielding performance compared to reported works.
4. Proposing a fabrication method which is cost-effective with no postprocessing requirements.

All these points were highlighted in the revised manuscript.

Comment 12:

The authors should prepare TEM and HRTEM images for detailed investigation of structure and morphology of samples.

Answer to comment 12:

We were not able to conduct the TEM and HRTEM measurements for our samples because some experiments and manpower were reduced during the summer vacation period ending in September. Nevertheless, the SEM images presented and discussed in Section 4.1 yet allow us to conclude about the presence of an interconnected network of carbon nanotubes that ensures a sufficient level of conductivity, yielding an excellent shielding effectiveness level.

Comment 13:

This work should be compared with the other work in Table form.

Answer to comment 13:

As already indicated in our response to Comment 9, our SE_T results were compared with previously published studies in Table 2.

Comment 14:

The novelty of this study should be inserted in the text clearly.

Answer to comment 14:

The novelty has been inserted clearly in the text, as previously explained in our answer to Comment 3 and 11, please see above.

Comment 15:

Where is the practical application of this manuscript? It must be added.

Answer to comment 15:

The practical application of this work has been clearly added to several places in the introduction:

"Additionally, polymer composites showed outstanding EMI shielding performance for construction, aerospace, electronics, and medical market"

"Several applications are covered in these frequency ranges, including marine communications in the 30 - 300 kHz, television, microwave, and mobile phones in the 300 MHz – 1 GHz, and satellite communications in the 10 – 26.5 GHz [5]."
"This research aims to fabricate and characterize CNT-PU samples for EMI shielding applications. These applications are applied in several industries such as microelectronics, computer, automotive, and aerospace."

Comment 16:
The discussion section is very short compared to the obtained results. Please go through it and add more comments and interpretations.

Answer to comment 16:
This comment looks similar to Comment 3 by the same reviewer. Please kindly refer to our answer to Comment 3 above.

Comment 17:
Please clearly mention the novelty of this work in the main parts of the article (introduction, method, results, and conclusion section).

Answer to comment 17:
This comment is very similar to Comment 4 by the same reviewer. Kindly refer to our answer to that comment above.

Comment 18:
All figures must be cleared (enlarge) and improved.

Answer to comment 18:
All figures were enlarged and improved.

Comment 19:
The figure caption should also include key experimental conditions and operating parameters. This applies to all figures.

Answer to comment 19:
All figures captions were modified.

Comment 20:
Please remake the scale bar in the images (figure 5) to make sure it is clear to read.

Answer to comment 20:
The positions of the scale bar in Figure 5 were changed to make it clear to read.

Additional change

During the revision of the manuscript, we noticed that equations (2-4) in the old version of the manuscript were wrongly applied to the calculation of SE_T, SE_A and SE_R previously shown in Figures 11 and 12. We apologize for this error and have replaced the wrong results with the correct ones for Figures 10 and 11 in the revised manuscript. This error does not affect the message delivered in our manuscript since the corrected results show higher values of shielding. We have also reorganized Figures 9 to 12 to enhance the readability and structure of the manuscript as requested by the reviewers. Figure 9 now shows return loss associated to S-parameter S_{11}, and Figure 10 shows SE_T associated to S-parameter S_{21}. The analysis of the contributions to SE_T and the EF distribution are now shown in Figures 11 and 12 respectively, in the revised manuscript.

Effects of carbon nanotubes on the AC conductivity, permittivity, and electromagnetic shielding performance of polyurethane foams in the 15 Hz – 26.5 GHz frequency range

Ahmad Mamoun Khamis[1*], Laetitia Urbanczyk[2], Christophe Detrembleur[2,3] and Isabelle Huynen[1]

[1] ICTEAM Institute, Université Catholique de Louvain, Louvain-la-Neuve, 1348 Belgium.

[2]Center for Education and Research on Macromolecules (CERM), CESAM Research Unit, University of Liege, Sart-Tilman B6a, 4000 Liege, Belgium.

[3]WEL Research Institute, avenue Pasteur, 6, 1300 Wavre, Belgium.

[*] Corresponding author: Ahmad.khamis@uclouvain.be.

Abstract

This study investigates the impact of increasing carbon nanotube (CNT) concentration on the AC conductivity, dielectric, and electromagnetic shielding properties of polyurethane (PU) foams. Four CNT-PU foam samples with different CNT contents (1 wt.%, 2.3 wt.%, 6 wt.%, and 11.2 wt.%) were fabricated using the dip coating method. Three different measurement techniques were employed to characterize the AC conductivity and complex permittivity of the CNT-PU composites across various frequency ranges (kHz, MHz, and GHz). COMSOL software was also used to calculate the scattering parameters and visualise the electric field distribution. The microstructure SEM images of CNT-PU samples confirmed that the CNTs formed interconnected and well-distributed networks on the PU surface skeleton, leading to conductive pathways that boost the absorption loss. Therefore, increasing CNT content increased the permittivity and conductivity of CNT-PU samples, and consequently, the total shielding effectiveness (SE_T). The incorporation of 11.2 wt.% CNT greatly enhanced the AC conductivity, increasing it from 3.6×10^{-6} S/cm (pure PU) to 0.0068 S/cm at 10 MHz. Furthermore, the corresponding values of complex permittivity also increased from 1.32 – j 0.0059 to 8.65 – j 3.7 at 1000 MHz. The complex permittivity of 11.2 wt.% CNT sample was 3.76 – j 3.56 at 25 GHz. The samples with 6 wt.% CNT and 11.2 wt.% CNT met the standard requirements for the electromagnetic interference shielding applications because their total shielding effectiveness (SE_T) values surpassed the 20 dB threshold within the 18 – 26.5 GHz frequency range. The visualization of the electric field distribution further confirmed that the 11.2 wt.% CNT sample greatly attenuated the electric field propagation through the material. The contribution of the absorption loss mechanism to the SE_T of CNT-PU samples surpassed 94% in the 18 – 26.5 GHz frequency range, indicating that the absorption loss was the main shielding mechanism in our samples.

Keywords

Carbon nanotubes, polyurethane, permittivity, numerical simulation, shielding effectiveness, microwave absorption.

1- Introduction

Electromagnetic interference (EMI) is a critical problem for communication systems and modern electronic devices, often causing reduced performance, data corruption, and malfunction [1]. EMI is created by external electromagnetic (EM) waves that interrupt the standard operation of electronic devices. Therefore, it is crucial to develop EMI shielding materials that can operate over a wide range of sectors such as aerospace, medical, electronics, defense, and automotive [2]. Metals are conventionally used for EMI shielding because of their high conductivity. Nevertheless, they are heavy, hard to process, and vulnerable to corrosion [3]. Therefore, polymer composites have emerged as an alternative solution to the metal-based EMI shielding. The advantage of polymer-based composites, compared to metal materials, is the manufacturing process that enables the production of complex shapes with lower density, leading to lower fuel consumption (for automobile and aviation) and higher speed in competitive sport [4]. Additionally, polymer composites showed outstanding EMI shielding performance for construction, aerospace, electronics, and medical market [5]. It is challenging to design conductive polymer composites (CPCs) because over-shielding leads to higher sample cost, while under-shielding could cause a product failure. There are three mechanisms involved in EMI shielding: absorption, reflection and multiple reflections. Absorption depends on the shield's thickness, and it increases with increasing concentration of magnetic or electrical dipoles that can dissipate the EM energy. The reflection is the primary shielding mechanism in a homogeneous conductive material, and the multiple reflection is the internal reflection within the shielding sample [6]. Conductive fillers such as carbon black, carbon nanotube (CNT) [7], graphite, and graphene [8] are added to polymers to form the conductive polymer composites.

In the 21st century, nanotechnology is considered one of the most promising techniques. This technology involves transforming the nanoscience theories of into practical applications by controlling, assembling, manipulating, and manufacturing samples at the nanoscale [9]. Nanostructure refers to structures or materials which have at least one dimension between 1 and 100 nm. These structures are fabricated using simple and complicated methods [10]. The very rapid development of nanoscience confirms that the manufacturing at the nanoscale will be integrated into all fields of technology and science. With development in science and technology, researchers embrace products and technologies which are cheaper, cleaner and safer than previous technologies [11]. Currently, nanotechnology is widely used in several industries and fields such as electronics, medicine, printing, textiles, agriculture, automotive, construction, and renewable energy [12]. A wide variety of nanomaterials have recently been developed for various applications such as sensing, catalysis, optoelectronics, and electronics [13]. In this study, carbon nanotubes were used to prepare the samples because their fibrous structures with high-aspect ratios are suitable as EMI shielding materials [14]. In addition, the polymer foams are widely used in many applications such as protective equipment, furniture cushioning, packaging of food, thermal insulation of medical devices, and transportation [15]. The CNT fillers can be incorporated into different polymers for EMI shielding applications, such as polypropylene (PP) [6], isotactic PP, high-density polyethylene (HDPE) [16], PU foam [17], polycarbonate (PC) [18], polycaprolactone (PCL) [19], and polylactic acid (PLA) [20]. However, PU foam is used in this study because it has unique properties such as low weight, low cost, and porosity, that influences the multireflection of EM waves inside the material [21]. The conductive PU composites can also be found in other applications, such as environmental and medical sensing, electrochemical energy storage, and tissue regeneration [22]. Additionally, the CNT-PU nanocomposites have been studied in various fields such as bone substitution, cardiovascular applications, ligament, tendon, and neural tissue engineering [23]. The CNT-foam samples can be fabricated using two main methods. In the first one, which is called the bottom-up method, the CNTs are directly dispersed to the polymer matrix, followed by the foaming process. In the second method, the CNTs are deposited (dip coating) onto a ready-made foam sample [24]. In this research, the latter method was used to fabricate the CNT-PU foam samples.

The electromagnetic properties of CNT-PU foams, fabricated via the bottom-up method, were studied in different frequency ranges such as 10^2 – 10^6 Hz [25], 30 MHz – 1.5 GHz [26], and 2 – 18 GHz [27]. On the other hand, studies on CNT-PU samples, prepared using the second method, focused on the engineering scaffolds [28], wearable pressure sensors [29], and damping applications [30]. It is important to note that the number of EM applications (such as EMI shielding) in which a certain material can be used depends on its EM properties at specific frequency ranges. Therefore, investigating the EM properties over a broad frequency range will increase the number of applications where the material may be used, compared to a narrow frequency range. This study investigates the interaction between the EM waves and CNT-PU samples, prepared using the second method, in three different frequency ranges (kHz, MHz, and GHz). Several applications are covered in these frequency ranges, including marine communications in the 30 - 300 kHz range, television, microwave, and mobile phones in the 300 MHz – 1 GHz range, and satellite communications in the 10 – 26.5 GHz range [5]. Therefore, three different setups were used to characterise the samples. Such characterizations are crucial for enabling CNT-PU samples to be used in a wide range of frequencies. To the best of our knowledge, foamed samples have never been characterized using the Dielectric Material Test Fixture (DMTF) because the upper electrode always presses the material under test (MUT). Such pressing decreases the thickness of the foam sample under test, leading to the following problems: the content of air inside the foam sample will decrease, which may result in wrong values of dielectric constant; it is not possible to measure the new thickness of the foam sample after the upper electrode presses the foam sample, and finally it is not possible to obtain the real dielectric constant of the MUT since a significant change in dimensions occurred. Thus, we developed a 3D holder to maintain a constant distance of 2.5 mm between the upper and lower electrodes, which will overcome the limitations of characterizing foam samples using DMTF. Therefore, this study presents, for the first time, the characterizations of foam samples using DMTF.

This research aims to fabricate and characterize CNT-PU samples for EMI shielding applications. These applications are applied in several industries such as microelectronics, computer, automotive, and aerospace [5]. The novelty of this work lies in the following aspects: 1- The usage of DMTF to characterize foam samples. 2- Investigating the electromagnetic properties of CNT-PU foam samples over a broad frequency range from 15 Hz to 26.5 GHz. 3- Visualizing the effects of increasing CNT concentrations on the electric field distribution of CNT-PU samples. The AC conductivity of CNT-PU samples is studied in the 15 Hz to 10 MHz frequency range. The permittivity results are also presented in the 10 MHz – 1 GHz and 10 – 25 GHz frequency ranges. In addition, COMSOL Multiphysics was used to calculate the scattering parameters (S_{11} and S_{21}) and visualize the electric field distribution (EFD) of CNT-PU samples in the 18 – 26.5 GHz frequency range. The impact of CNT concentrations on the EFD inside CNT-PU samples has not been studied previously using COMSOL. Five simulations were conducted to investigate the effects of CNTs content on the intensity and distribution of the electric field.

2- Materials and methods

2.1 Materials

Two materials were used in the fabrication of the CNT-PU foam samples:

1- AQUACYL™ AQ0303 waterborne dispersions of multiwall carbon nanotubes (Nanocyl SA, Sambreville, Belgium).

2- Open-cell polyurethane foam with a net density of 54 Kg/m^3 (SiPLA SA, Wavre, Belgium). The average pore diameter is around 0.46 mm.

2.2 Fabrications of CNT-PU samples

In this study, the dip coating method is chosen for the fabrication of CNT-PU foam samples because of three advantages: it is the most cost-effective, the fabricated foam can be used directly without post-processing, and finally the foam is fully covered with the applied nanofiller. The dip coating method has been used in previous studies to coat foam samples with different fillers [31, 32]. The commercial CNT/water masterbatch Aquacyl 0303 was diluted with distilled water at specific ratios to prepare four different CNT solutions. The dilution factors used were 1/40, 1/20, 1/10 and 1/4 for a total volume of 1200 ml. Then, the pure PU foam was immersed in the diluted CNT solution for twenty-four hours. A weight of 1 kg was applied to the foam's surface to immerse the sample, and it was squeezed 5 times during the first hour to enhance the penetration of liquid inside the foam. Afterwards, the sample was removed and dried in a vacuum oven for twenty-four hours at 70°C. The weight difference between before and after the dipping process was used to deduce the amount of CNT incorporated into the PU foam. This procedure led to CNT-PU foam samples containing different CNT concentrations (1 wt.%, 2.3 wt.%, 6 wt.%, and 11.2 wt.%). The surface dimensions of each sample were (16 cm x 16 cm) with a thickness of 2 cm. Samples were prepared in a rigorous manner. The CNT concentration is estimated with 5% error due to the balance precision of 0.01 grams used.

3- Characterization and simulation methods

All measurements were performed at room temperature (22.5 °C). The scanning electron microscope (SEM) was used to examine the morphology of CNT-PU samples. Novocontrol was used to characterize the AC conductivity. The impedance analyser and vector network analyser were used to characterize the permittivity.

COMSOL Multiphysics software was used to obtain scattering parameters and electric field distributions. Characterizing of CNT-PU samples, over a broad frequency range using multiple measurement techniques is a key novelty of this study.

3.1 Morphology, AC conductivity, and permittivity measurements

The dispersion of CNTs on the surface of PU was investigated using JEOL 7600F SEM (operating at 15 keV). The CNT-PU samples were coated with a gold layer using the Cressington sputter 208HR.

The AC conductivity of CNT-PU samples was measured in the 15 Hz to 10 MHz frequency range using Alpha-A Analyzer (Novocontrol) connected to a Dielectric Test Fixture (Agilent, 16451B). This system uses the parallel plate method that sandwiches the MUT between two electrodes to form a capacitor [33] as shown in Fig.1. The measurements were conducted using Novocontrol Windows-based WinDETA software, which supports dielectric, impedance, conductivity, and gain phase measurements. The accuracy of the results was validated by measuring a reference material (PTFE) before conducting the measurement on the CNT-PU samples. The thickness of each sample was 4 mm. The uncertainty in the sample geometry was provided by the manufacturer as follows: for a sample with a thickness of 0.1 mm, the error in the thickness has to be less than 1 µm for a 1% accurate result.

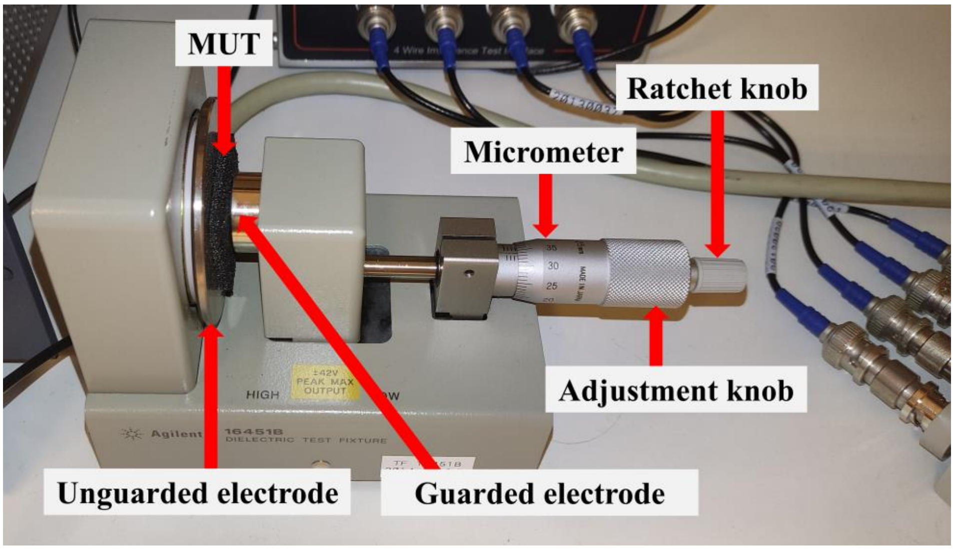

Fig. 1: Dielectric Test Fixture setup for AC conductivity measurements in the 15 Hz to 10 MHz frequency range.

The Dielectric Material Test Fixture (Keysight, 16453A) connected to the Impedance Analyzer (Keysight, E4991B) was used to measure the relative permittivity (ε' – jε") of CNT-PU samples in the 10 MHz - 1 GHz frequency range at room temperature (22.5 °C). The measurement setup is presented in Fig. 2. This test fixture employs the parallel plate capacitor method [34]. Calibration was performed in three stages: open, short, and load. In the first stage (open), the knob was pulled up and the latch button was pressed while holding up the knob. The second stage was performed after releasing the latch button, so the upper electrode contacted the lower one. A PTFE sample with 0.770 mm thickness was used as a load to perform the third stage of calibration. It was also used as a reference material to confirm the calibration accuracy. Initially, it was not possible to measure the foamed CNT-PU samples using the standard DMTF because the upper electrode always compresses the MUT, which cannot keep its initial thickness and air content. Hence, we designed a novel 3D holder to keep the knob holding up. With the 3D holder in place, the distance between the electrodes matched the samples' thickness of 2.5 mm.

Measurement accuracy of the impedance analyzer applies when the calibration is performed at 23 °C ± 5 °C. When the calibration is below 18 °C or above 28 °C, the measurement error doubles. The basic accuracy is ±0.65% and the impedance range is 120 mΩ to 52 kΩ (10% measurement accuracy range).

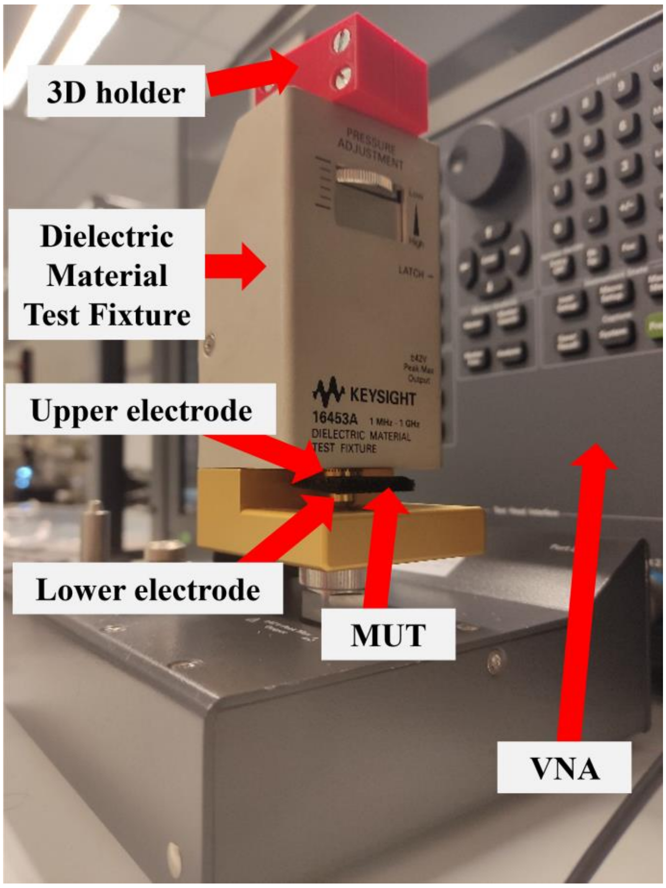

Fig. 2: Keysight impedance analyser connected to the DMTF for permittivity measurements in the 10 MHz - 1 GHz frequency range.

The relative permittivity (ε' – j ε") of CNT-PU samples was measured using the vector network analyzer (VNA, Keysight, N5242B) connected to an OECP (Performance probe kit) in the 10 – 25 GHz frequency range. The typical power level accuracy (dB) of the VNA is ± 0.60 for the 10 – 18 GHz frequency range. The Agilent (N4691) Electronic Calibration (ECal) was connected in line between the OECP and the VNA, as shown in Fig. 3. The "Coaxial Probe Method" option was selected in the Keysight Materials Measurement Suite. The calibration stages were as follows: Open, short, and distilled water, for 201 points, at room temperature (22.5 °C). After performing the calibration, two different reference materials (water and isopropanol) were used to validate the calibration accuracy. The measurements of CNT-PU samples were conducted with free-gap contact between the MUT and the probe.

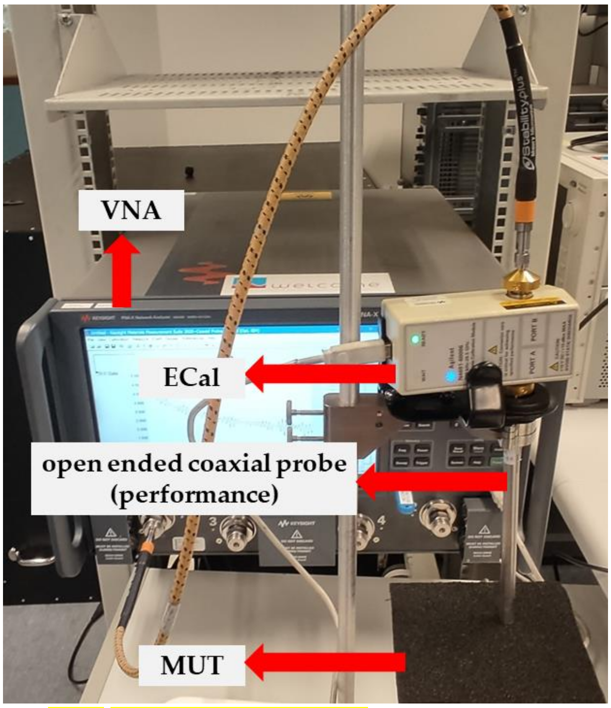

Fig. 3: Keysight N5242B VNA connected to an OECP for permittivity measurements in the 10 – 25 GHz frequency range.

3.2 COMSOL simulations

COMSOL Multiphysics 6.2 is a Finite Element Method (FEM) software. The FEM divides the continuous spatial domain under scope into a finite number of small modules, set up each module of the formula and solve it, then combine them [35]. In our study, the permittivity values of CNT-PU samples measured using the VNA connected to the OECP were used to calculate the scattering parameters (S_{11} and S_{21}) and visualize the electric field distribution using COMSOL. The simulated WR42 waveguide has the dimensions of 1.0668 cm x 0.4318 cm [36], and it covers the 18 – 26.5 GHz frequency range. The waveguide geometry was divided into three sections as shown in Fig. 4, where a sample thickness of 1 cm is considered.

The process for building and simulating the CNT-PU geometry was conducted using the following steps. The Model Wizard with 3D model was selected. Then, the Radio Frequency module with Electromagnetic Waves and Frequency Domain was assigned. Next step, the geometry was built using the Geometry interface, and the EM properties were stated in Materials. The boundary conditions were then introduced as Perfect Electric Conductor, and the two ports were defined. The meshing was generated with Finer element size for higher accuracy, before configuring the frequency range and executing the study (Compute). Finally, the results were exported in terms of scattering parameters and electric field distribution.

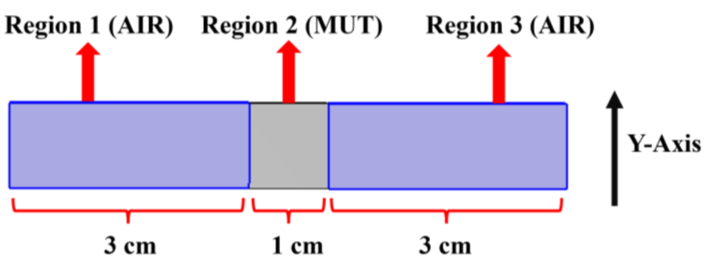

Fig. 4: The waveguide regions in COMSOL simulation.

4- Results and discussions

This section presents the surface morphology examined using SEM, AC conductivity measured using Novocontrol system connected to a Dielectric Test Fixture in the 15 Hz - 10 MHz frequency range, complex permittivity characterized using an impedance analyzer connected to a DMTF and VNA system connected an OECP in the frequency ranges of 10 – 1000 MHz and 10 – 25 GHz, respectively. The scattering parameters obtained using COMSOL Multiphysics are also presented, together with the related SE_T calculations and EFD visualization.

4.1 Surface morphology of CNT-PU samples

The SEM was used to examine the morphology of CNT-PU composites. The SEM images, shown in Fig. 5, shared the same magnification scale of 50k. The PU matrix exhibits a smooth skeleton as also reported in the previous study [37]. The gold coating, described in Section 3.1, caused the cracks visible in Fig. 5.a. The CNTs are clearly visible and evenly distributed on the samples' surfaces with no accumulation, as shown in the images of Fig. 5 (b, c, d, and e). These images also do not show the PU surfaces, proving that the CNT network covered all PU surfaces in the CNT-PU samples without interruption. The images of CNT-PU samples also confirm that the CNT fillers are not isolated. Furthermore, the CNTs were intertwined with each other to establish interconnected networks as presented in the images of Fig. 5 (b, c, d, and e). The conductive path of CNT-polymer composites is established by CNTs that are in contact with each other [38]. The SEM images of our CNT-PU samples confirm that the CNTs are in contact together, leading to a conductive path on the surface. The interconnected networks were successfully formed in the 1 wt.% CNT specimen that had the lowest concentration of CNT. Therefore, we cannot see a noticeable change in morphology with increasing CNT content because the SEM only examines the sample's surface. Hence, increasing the CNT content leads to denser conductive networks of CNT. Consequently, the greatest rise in conductivity, complex permittivity, and SE_T, presented in the subsections below, was recorded between the two samples of PU and 1 wt.% CNT. This is because the percolated networks of CNT were already built at 1 wt.% CNT sample, leading to an uninterrupted conductive pathway.

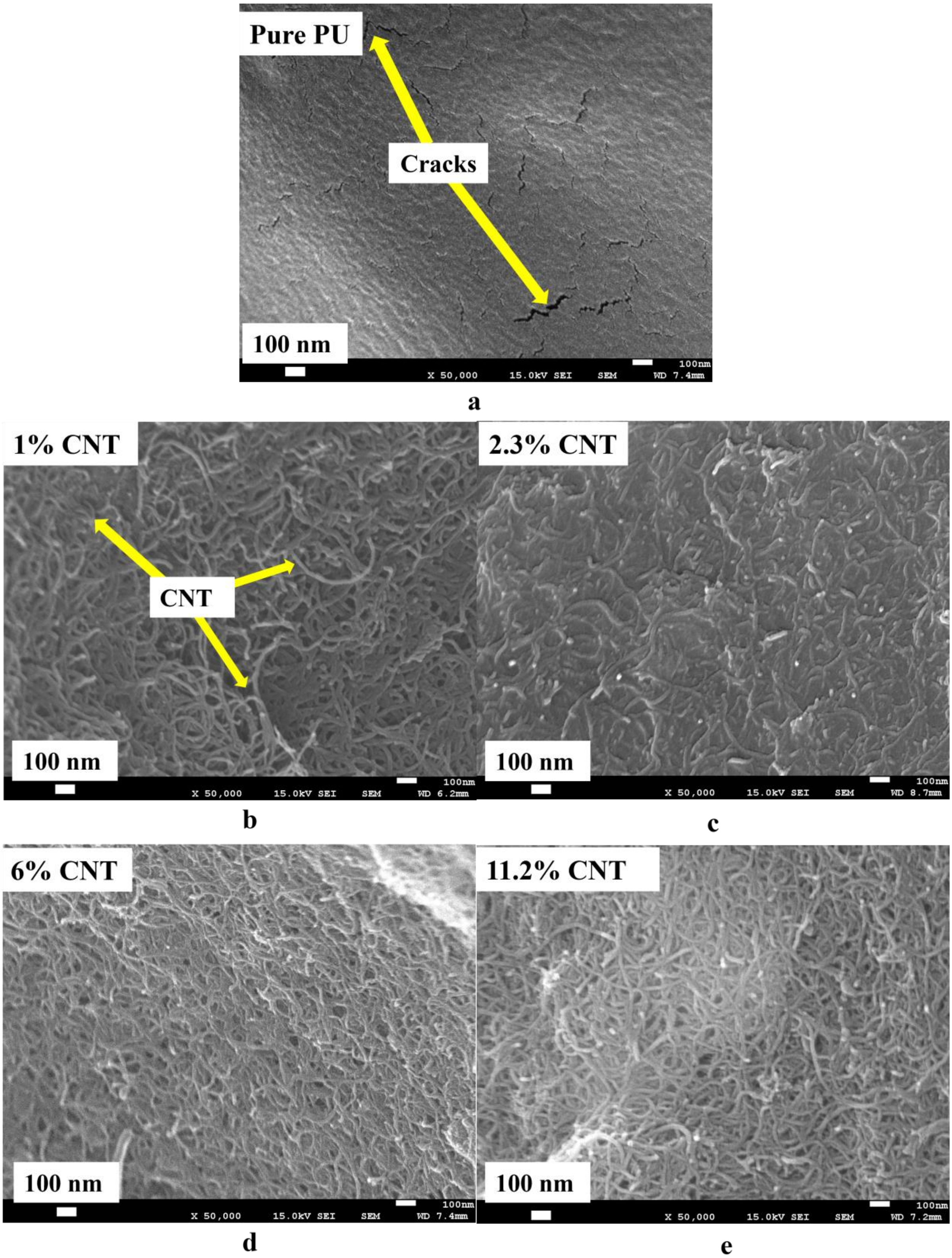

Fig. 5: SEM images of CNT-PU samples, obtained using JEOL 7600F SEM (operating at 15 keV); a: PU, b: 1 wt.% CNT, c: 2.3 wt.% CNT, d: 6 wt.% CNT, e: 11.2 wt.% CNT.

4.2 AC conductivity in the 15 Hz - 10 MHz frequency range

The AC conductivity (σ_{ac}) of CNT-PU samples measured using the Novocontrol Analyzer in the 15 Hz-10 MHz frequency range is shown in Fig. 6. In this frequency range, the ohmic conduction dominates the electrical response below 100 kHz [39]. Increasing CNT contents significantly enhanced the σ_{ac}. At 10 MHz, the AC conductivity values of neat PU (no fillers) and 11.2 wt.% CNT samples were 3.6×10^{-6} S/cm and 0.0068 S/cm, respectively, which means that the σ_{ac} increased by more than 1800 times. These results are consistent with a study conducted by Hoang [40]. Ilya also reported that the AC conductivity of PU is approximately 10^{-6} S/cm within the 10^5-10^6 frequency range [41].Our CNT-PU samples are less conductive than copper since they did not reach the value of 1000 S/cm; however, they are not insulators because their AC conductivity is higher than 10^{-8} S/cm [42].

At 10 MHz, the σ_{ac} values were 0.00048 S/cm, 0.0012 S/cm, 0.0037 S/cm, and 0.0068 S/cm for the 1 wt.% CNT, 2.3 wt.%, 6 wt.%, and 11.2 wt.% samples, respectively. This indicates that the σ_{ac} increased by 150%, 208%, and 83% by increasing the CNT concentration from 1 wt.% to 2.3%, 2.3 wt.% to 6 wt.%, and 6 wt.% to 11.2 wt.%, respectively.

The AC conductivity is directly related to the frequency (f) and the imaginary part of permittivity (ε'') via the following equation [43]:

$$\sigma_{ac} = 2\,\pi\,\varepsilon_0 f\,\varepsilon'' \quad (1)$$

Where ε_0 represents the free space permittivity. Based on Equation 1, the σ_{ac} is directly proportional to f and ε''. Increasing CNT content in the samples thickened the CNT coatings on the surfaces, leading to additional conductive pathways which resulted in higher energy loss, ε'', and AC conductivity. The additional conductive pathways also impacted on the increment behaviour of AC conductivity with frequency, where a sharper rise in AC conductivity occurs in samples with higher CNT content.

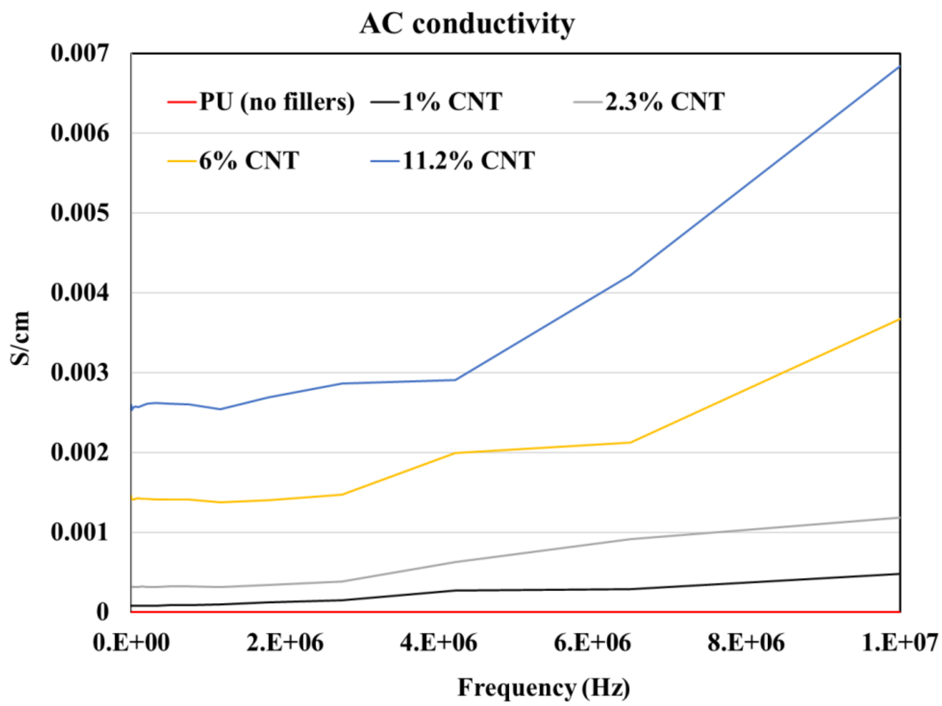

Fig. 6: AC conductivity of CNT-PU samples measured using Alpha-A Analyzer (Novocontrol) connected to Dielectric Test Fixture, employing the parallel plate method, in the 15 Hz-10 MHz frequency range.

4.3 Dielectric properties in the 10 – 1000 MHz frequency range

The real part of permittivity (dielectric constant, ε') indicates the amount of energy stored by a certain material in a specific electric field relative to empty space, while the imaginary part of permittivity (loss factor, ε") shows how much of this energy can be converted into heat [44]. The ε' and ε'' are key indicators for analysing the wave absorption performance of composite materials [45]. The presence of the conductive CNT fillers in the electrically insulating matrix of PU significantly increases the permittivity (ε' and ε") of CNT-PU samples, as shown in Fig. 7 and Table 1. The ε' values of PU sample reported in this study are in accordance with the ones reported by Wang [46].

There are four polarization mechanisms known in dielectric materials such as PU matrix: interfacial, dipole-oriented, ionic, and electronic. However, each mechanism corresponds to a certain frequency range. For example, the interfacial polarization takes place in the low-frequency range while the electronic polarization occurs in the optical frequency range around 10E15 Hz. Therefore, electronic polarization can be ignored in our study, but the effects of interfacial polarization could occur at the beginning of the MHz frequency range. In our samples, PU is a dielectric material while CNT is a conductive filler; therefore, the space charges accumulate at the interface between the CNT and PU contribute to the interfacial polarization (Maxwell–Wagner–Sillar) [47]. It is worth noting that the interfacial polarization in our samples may occur at the interface between PU and CNTs because a surface layer of CNTs was formed on the PU surface as confirmed in Section 4.1. The high permittivity at lower frequencies could be due to free charge built up at the interface between PU and CNT. Therefore, the permittivity decreased with increasing frequency because the periodic reversal of the electric field occurred so fast that there was no excess charge in the direction of the field, leading to a decrease in the interfacial polarization due to the charge accumulation decrement [48]. The PU has covalent bonds; therefore, the ionic polarization can also be excluded in this study. Dipole polarization could be dominant in our study because the urethane [-NH-CO-O-] group, which is the main building block of PU, exhibits a dipole moment. However, the permittivity of PU, shown in Fig. 7, is constant over the whole frequency range, which suggests that the dipolar relaxation took place below the measured frequency range. Moreover, the dielectric constant of PU, 1 wt.% CNT, and 2.3 wt.% CNT samples, shown in Fig. 7, is nearly frequency independent compared to 6 wt.% CNT and 11.2 wt.% CNT samples which are strongly dependent on frequency below 0.5 GHz. This is explained by the high concentration of CNT, which causes a denser conductive network, leading to stronger interfacial polarization.

The imaginary part of permittivity also increased with increasing CNT content, in agreement with the increment in the AC conductivity as presented in Fig. 6. This observation follows the study by Huang [49]. EM waves convert into electric currents that are resisted by the absorber, generating joule heat that dissipates the EM wave energy [50]. In our study, the presence of the interconnected network of CNT fillers was confirmed in Section 4.1. Hence, increasing the CNT content increased the dissipation of EM wave energy due to the increment in conductivity.

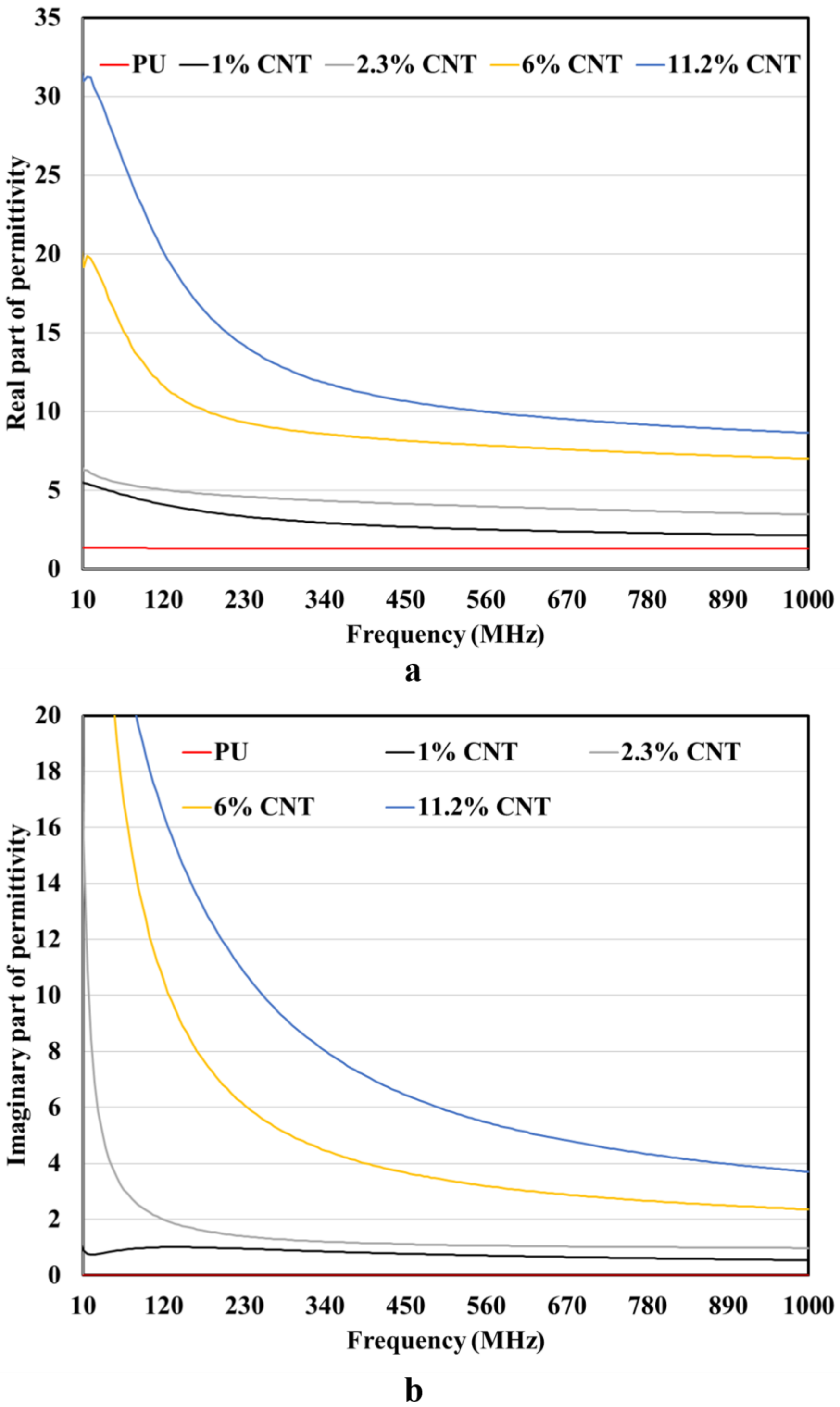

Fig. 7: Permittivity of CNT-PU samples measured using impedance analyzer E4991B connected to the DMTF (parallel plate method) in the 10 MHz – 1000 MHz frequency range. a: real part; b: imaginary part.

Table 1: Complex permittivity of CNT-PU samples at 1000 MHz, obtained using the impedance analyzer.

Sample name	Complex permittivity at 1000 MHz	
	Real part	Imaginary part
PU	1.32	0.0059
1 wt.% CNT	2.14	0.55
2.3 wt.% CNT	3.47	0.98
6 wt.% CNT	7.01	2.36
11.2 wt.% CNT	8.65	3.70

4.4 Dielectric properties in the 10 GHz – 25 GHz frequency range

The real and imaginary parts of permittivity for the CNT-PU samples in the 10 – 25 GHz frequency range are shown in Fig. 8. The ε' and ε" of 6 wt.% and 11.2 wt.% CNT samples continued to decrease with increasing frequency, which can also be attributed to the denser (additional) conductive networks of CNT as described in Section 4.1. It is important to note that the cause for the permittivity decrement with frequency in Fig. 7 (MHz range) and Fig. 8 (GHz range) may not have the same origin. The increment of permittivity with CNT concentrations could be explained by the increment of conductivity since CNT is symmetric and does not have dipole moments [51]. Therefore, the impact of dipole polarization in the CNT structure could be neglected, despite that some local dipoles could arise from curvature or defects.

At 25 GHz, the ε' values were 1.37, 1.86, 2.39, and 3.76 for the 1 wt.%, 2.3 wt.%, 6 wt.%, and 11.2 wt.% CNT samples while the corresponding values of ε" were 0.44, 0.82, 2.07, and 3.56, respectively. This indicates that the ε' and ε" increased by 36% and 86% with increasing the CNT concentration from 1 wt.% to 2.3 wt.%, respectively.

The relaxation time (τ) decreases as frequency increases; therefore, only certain polarization mechanisms with very low τ can contribute to the permittivity such as hopping and tunnelling. The electrons can tunnel from one CNT to another even when the separations between CNTs are in the order of a few nanometers [52]. The hopping and tunnelling rates could become slow to follow the quickly changing electric field, leading to a reduction in permittivity with frequency above 10 GHz, especially in 11.2 wt.% CNT sample where the rates are very high. Furthermore, the decrement of permittivity with frequency in the 1 wt.% CNT and 2.3 wt.% CNT samples is minor because the hopping and tunnelling rates were initially low. The permittivity of PU continued its stable behaviour over the whole frequency range due to the absence of conductive charges.

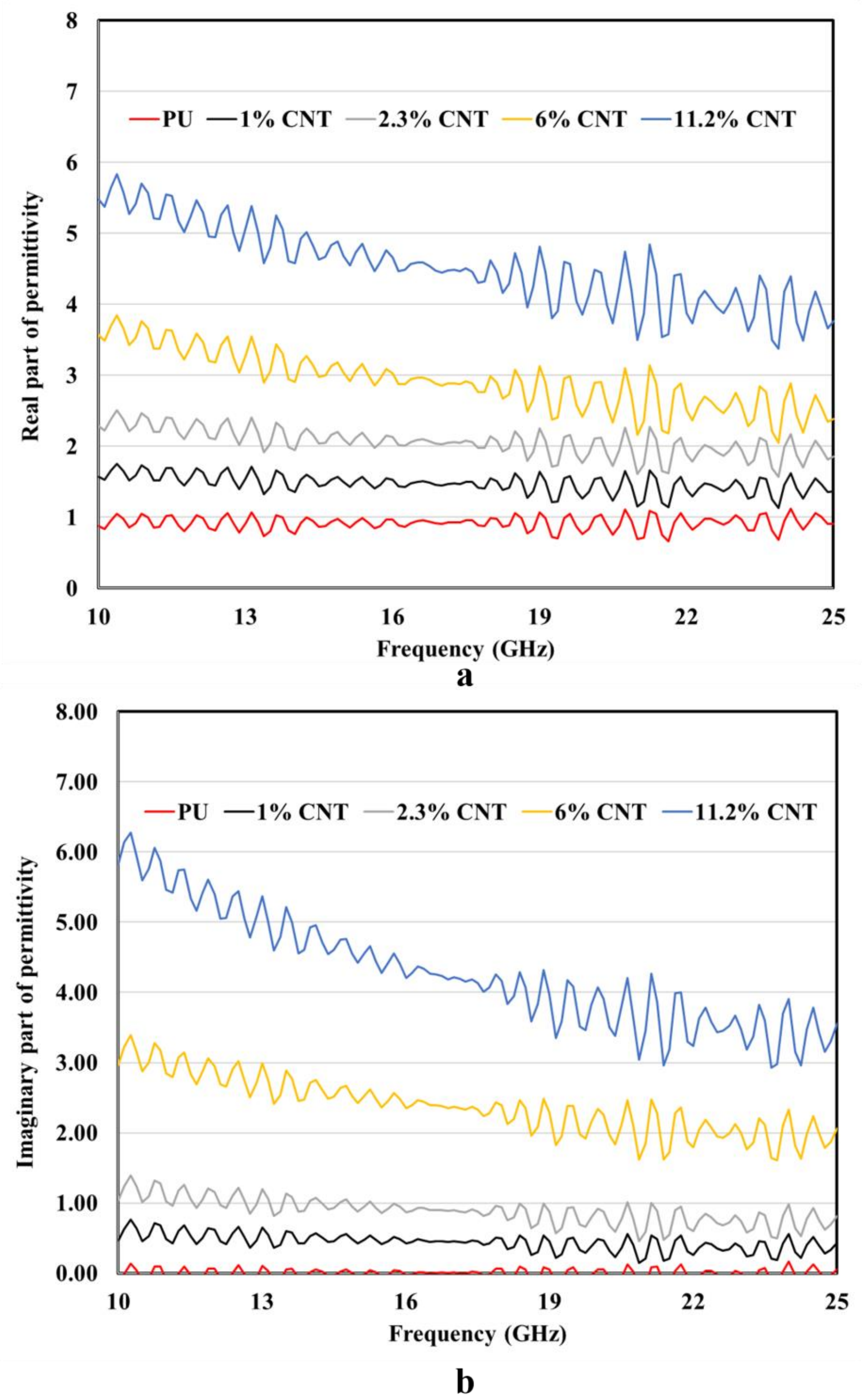

Fig. 8: Permittivity of CNT-PU samples measured using OECP connected to VNA (obtained using VNA connected to the OECP) in the 10 – 25 GHz frequency range. a: real part; b: imaginary part.

4.5 Electromagnetic shielding effectiveness and electric field distribution

The S_{11} (reflection coefficient) represents the power reflected to port 1, while the S_{21} (transmission coefficient) represents the power transferred from port 1 to port 2 [53]. S_{11} and S_{21} describe the interaction between EM waves and MUT. The scattering parameters (S_{11} and S_{21}) obtained using COMSOL software were used to calculate the return loss (*RL*), absorption loss (SE_A), reflection loss (SE_R), and total shielding effectiveness (SE_T) using the following equations:

$$RL = 10\log(S_{11}^2) \quad (2)$$

$$SE_A = -10\log((S_{21}^2) \div (1 - S_{11}^2)) \quad (3)$$

$$SE_R = -10\log(1 - S_{11}^2) \quad (4)$$

$$SE_T = SE_A + SE_R + SE_{MR} \quad (5)$$

Where the SE_{MR} represents the multiple internal reflections, which can be neglected when the total shielding effectiveness is higher than 10 dB [54].

Increasing the CNT content increased the electrical conductivity of the sample, resulting in higher EM reflection and consequently lower return loss, as shown in Figure 9. This finding is in agreement with the AC conductivity results presented in Fig. 6. The relationship between conductivity and the wave impedance can explain the increment in EM reflection (reduction in RL). The wave impedance (Z) equation is expressed as follows:

$$Z = ((j\omega\mu) \div (\sigma_{ac} + j\omega\varepsilon))^{0.5} \quad (6)$$

Where $\omega = 2\pi f$ represents the angular frequency of the wave, μ is the magnetic permeability, σ_{ac} is the electrical conductivity of the MUT, and ε is the (real) electric permittivity. The conductivity's increment caused a decrease in the wave impedance with respect to that of air, which in turn increased the EM reflection. Hence, more EM energy is reflected with higher CNT concentration because of the impedance mismatch. The RL values of PU, 1 wt.% CNT, 2.3 wt.% CNT, 6 wt.% CNT, and 11.2 wt.% CNT samples were -37.7 dB, -17.63 dB, -11.80 dB, -8.08 dB, and -6.07 dB, respectively. The PU sample had the lowest RL over the whole frequency range because of the good impedance matching between the free space and the PU sample (which has a low value of dielectric constant). On the contrary, increasing the CNT content resulted in higher values of dielectric constant, leading to higher impedance mismatching and consequently higher RL values.

At 26.5 GHz, the SE_T of PU, 1 wt.% CNT, 2.3 wt.% CNT, 6 wt.% CNT, and 11.2 wt.% CNT samples were 0.57 dB, 8.33 dB, 14.20 dB, 30.90 dB, and 42.84 dB, respectively. This means that increasing the CNT content from 0 wt.% CNT (PU) to 1% CNT enhanced the SE_T by around 1361% while the increment from 6 wt.% CNT to 11.2 wt.% only enhanced the SE_T by around 39%. The reason for this drop from 1361% to 39% could be because of the conductive network of CNT which was built on the 1 wt.% CNT sample, as confirmed in Subsection 4.2. Then, increasing the CNT content to the pre-built conductive network can slowly enhance the SE_T.

The SE_T of CNT-PU samples increased with increasing frequency and CNT content as shown in Fig. 10. The SE_T increment with increased CNT content can be attributed to the increase in AC conductivity which caused higher energy absorption. Additionally, increasing frequency causes higher ohmic loss per volume unit because the power (current) density normally increases with increasing frequency. Samples with higher CNT concentrations tend to block more EM waves due to the increment in absorption as explained in Subsection 4.3. It is also worth noting that increasing the content of CNT caused an increase in the ascending trend of SE_T values. The SE_T values of PU are almost constant compared to the ones of the 11.2 wt.% CNT sample that ascends steeply. This trend is attributed to the fact that EM waves tend to dissipate more when interacting with absorbing material at higher frequencies.

The good EMI shielding material causes a maximum attenuation of the EM wave by absorption or reflection with inappreciable transmission. When the SE_T of a certain material is 20 dB, this means that there is an attenuation of 99% of the total energy of the incident wave [55]. The EMI shielding requirements depend on the application. For example, the EMI shielding of 15-20 dB is considered an adequate level of shielding for desktop computers and laptops [56]. Our 6 wt.% CNT and 11.2 wt.% CNT samples meet and exceed the required value (20 dB) for the mentioned applications over the whole frequency range. Additionally, the shielding performance of CNT-PU samples can be enhanced by increasing the sample's thickness and/or CNT content.

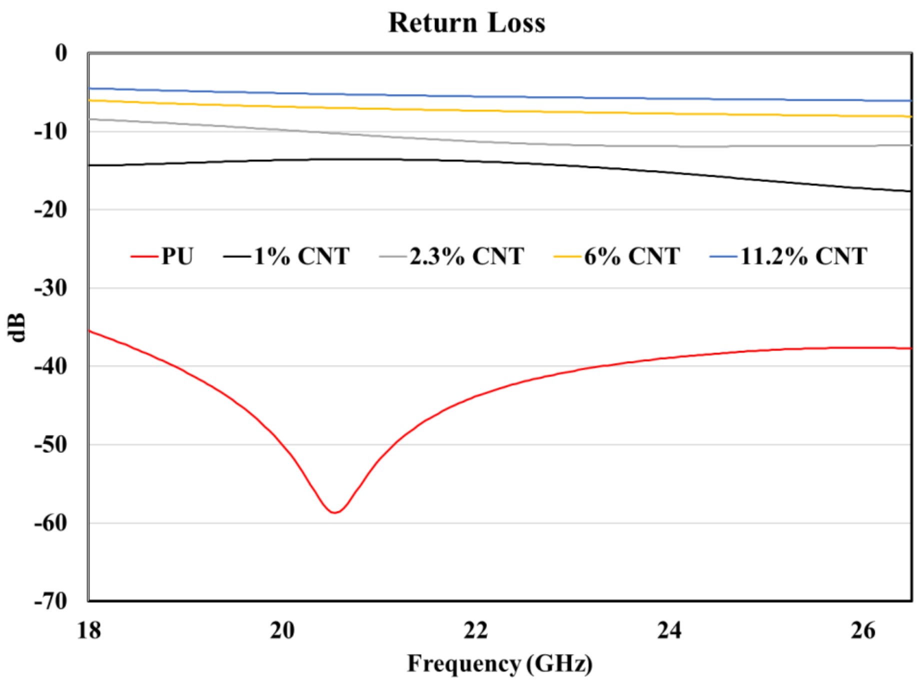

Fig. 9: Return loss of CNT-PU samples in the 18 – 26.5 GHz frequency range obtained using Equation 2.

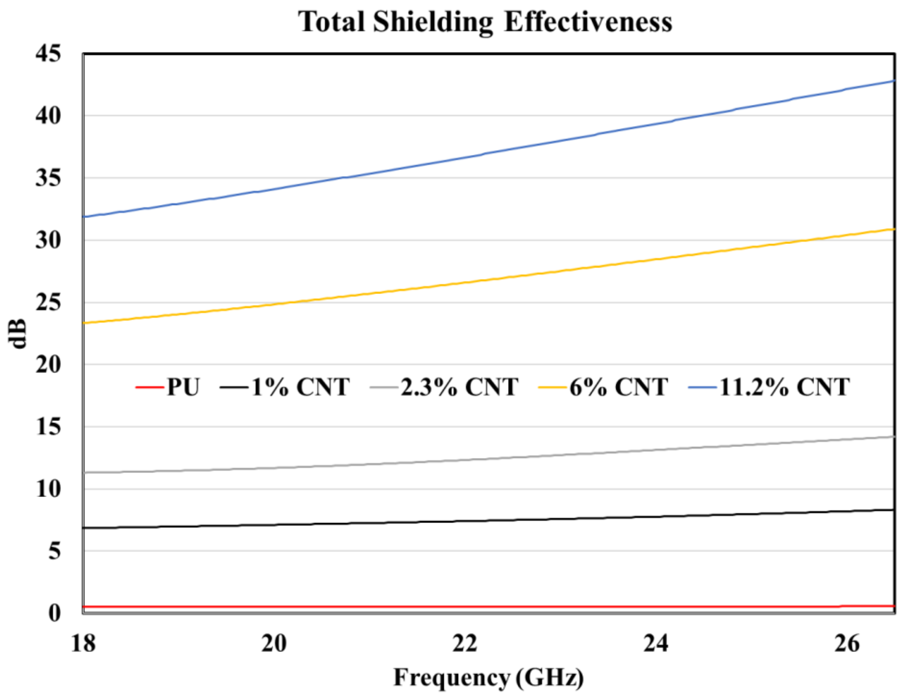

Fig. 10: Total shielding effectiveness of CNT-PU samples in the 18 – 26.5 GHz frequency range, obtained using Equation 5.

The contribution of reflection loss to the SE_T is not significant compared to the absorption loss which greatly influenced the SE_T of CNT-PU sample, as presented in Fig. 11. The SE_A contribution to the SE_T of CNT-PU samples was greater at higher frequencies. For example, the SE_A of 1 wt.% CNT sample caused around 97.6% of the SE_T at 18 GHz compared to 99.1% at 26.5 GHz. Such behaviour could be attributed to higher ohmic loss at higher frequencies, leading to higher absorption performance. Hence, our samples are highly preferred in industry because they reduce primary and secondary reflections that can cause unwanted EMI in nearby devices, eliminating the EMI and preventing it from spreading to the environment.

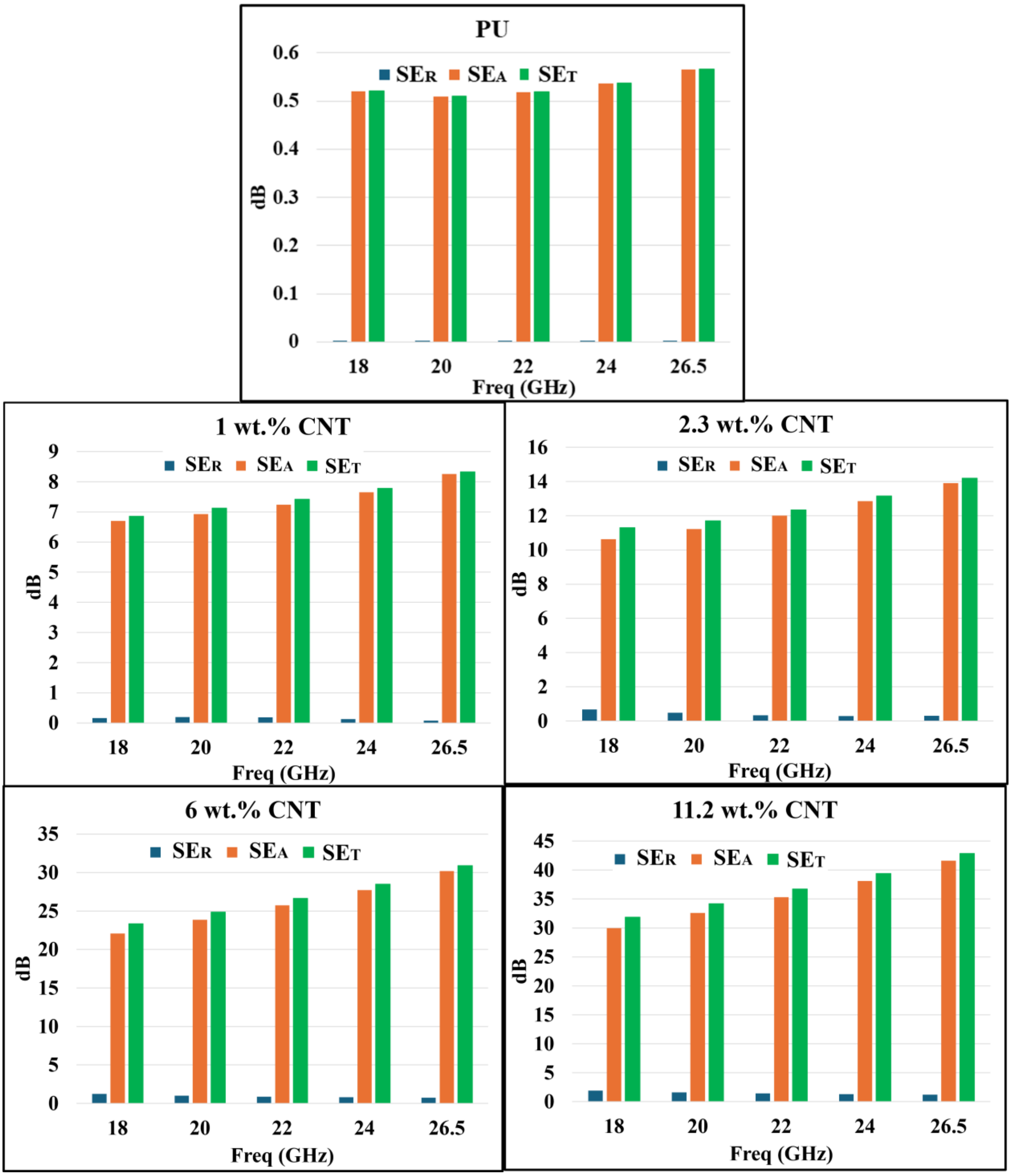

Fig. 11: The contribution of SE_R and SE_A to the SE_T of CNT-PU samples at certain frequencies of 18 GHz, 20 GHz, 22 GHz, 24 GHz, and 26.5 GHz, calculated using Equations 3-5.

The SE_T results obtained in this study were compared with previously published literature, as presented in Table 2. The SE_T results of our CNT-PU samples surpassed reported results, showing better EM shielding performance.

Table 2: The comparison of SE_T results with previous studies

Materials and filler percentage	Thickness (mm)	SE_T (dB)	Frequency (GHz)	Ref.
CNT/PU with 4.35% of CNT without buckling structures (UCNPF)	10	≈ 25	12	[57]

CNT-PU with 25% of CNT	2	≈ 30	12	[58]
CNT-PU with 9% of CNT	3.4	≈ 9	12	[59]
Polycarbonate - carbon nanotubes (PC-CNT) with 1% of CNT	5	≈ 8	18	[60]
polycarbonate - poly(styrene-*co*-acrylonitrile) (PC-SAN) with 3% of CNT	2	≈ 20	18	[61]
Polyethylene/Poly(vinylidene fluoride)/Fe_3O_4/Carbon nanotubes (PE/PVDF/Fe_3O_4/CNTs) with 10% CNT	2.6	≈ 29	26.5	[62]
CNT-PU with 6% CNT	10	30.9	26.5	This work
CNT-PU with 11.2% CNT	10	42.8	26.5	This work

The CNT concentrations had a significant impact on the electric field (EF) distribution as presented in Fig. 12. The Y axis ranges from - 40 mm to 30 mm. The MUT represents the region from -10 mm to 0 mm. There was a big change in the EF behaviour in region 3 compared to region 1 for the CNT samples. However, the PU sample did not have a strong impact on the EF, which only countered a slight decrease in intensity. This pattern can be explained by the weak interaction between the electric field and pure PU sample. The permittivity values of PU sample, presented in Figs. 7 and 8, are close to one of free space, leading to a negligible dielectric loss. Therefore, the EF can pass through the PU sample with a very weak attenuation. On the other hand, the intensity of the EF in region 3 decreased with increasing the CNT content which enhanced the AC conductivity and caused more interaction with the EF. The permittivity results shown in Figs. 7 and 8 are consistent with the EF distribution shown in Fig. 12. Samples with higher permittivity attenuated the EM signal more effectively, leading to a lower EF in region 3 as the CNT content increased. The EF could not enter the 11.2 wt.% sample because it had the highest concentration of CNT, which causes more reflection and losses. The regions of strong electric are totally separated in the 11.2 wt.% CNT samples compared to the 1 wt.% CNT sample where the regions of strong EF are connected to each other with lower values (around 5 × 10^3 V/m). Increasing the content of CNT caused more concentrations of the electric field at specific regions.

The EF distribution analysis can help in designing EM shielding materials such as electronic packaging, electrical enclosures, and gaskets. Such simulations are important before producing the prototype to predict the failures that could lead to an extensive EF in some regions. The EMI shielding material is usually classified as low quality if the EF intensity is slightly decreased after passing through it, compared to a high-quality shielding material, which strongly decreases the EF intensity. These simulations can enhance the design accuracy and reduce the fabrication cost, leading to optimal EMI shielding materials.

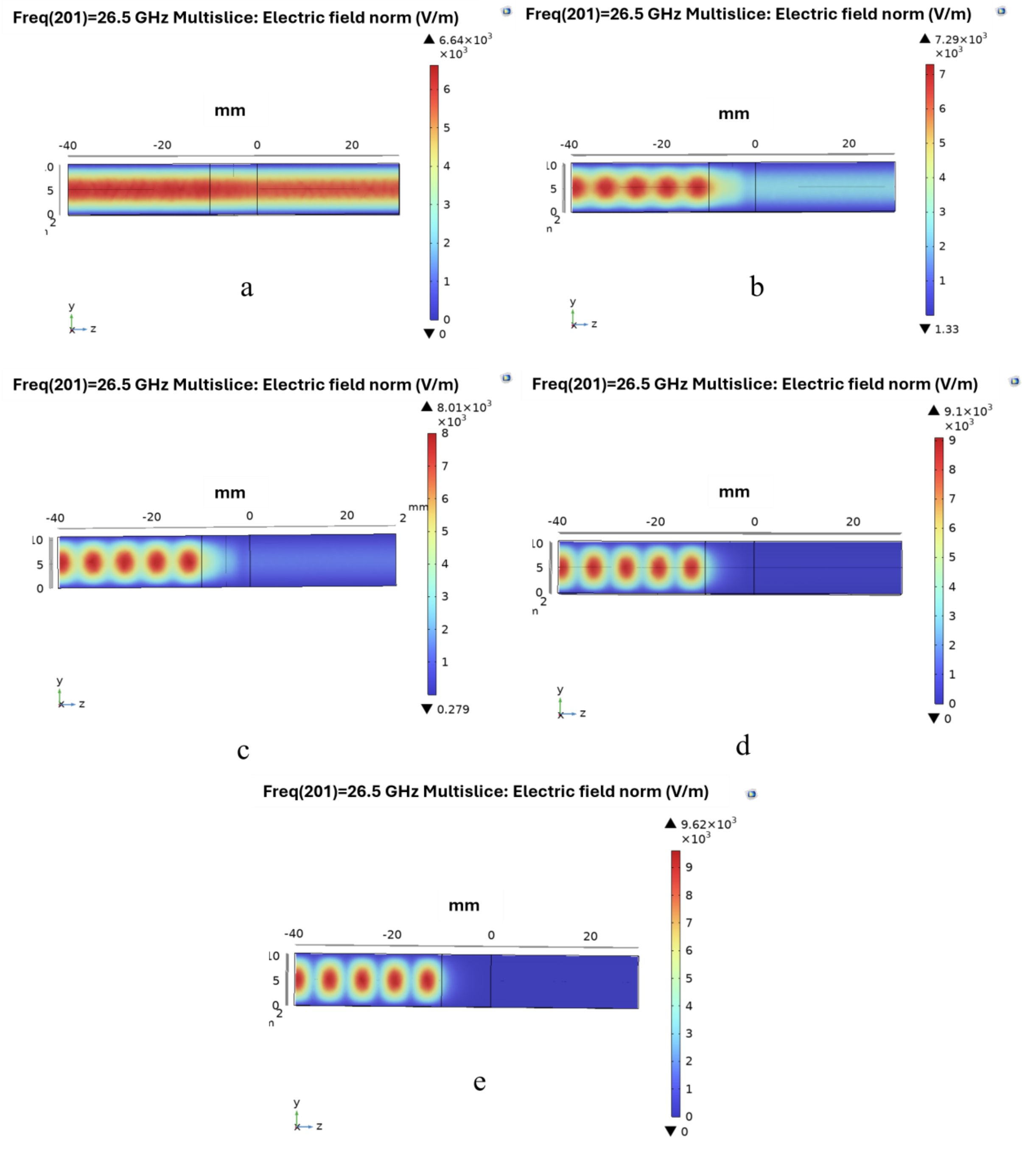

Fig. 12: Electric field distribution obtained using COMSOL Multiphysics at 26.5 GHz. a: PU sample, b: 1 wt.% CNT, c: 2.3 wt.% CNT, d: 6 wt.% CNT and e: 11.2 wt.% CNT.

5- Conclusion

CNT-PU foam nanocomposites with different CNT contents were successfully prepared and characterized for absorption-based EM shielding applications. The measurements were conducted over a broad range of frequencies to cover a wide range of applications. The impact of increasing the CNT content on the AC conductivity and permittivity was investigated using different measurement techniques. Additionally, the effects of CNT content on the scattering parameters (S_{11}, S_{21}) and the intensity of electric field distribution of CNT-PU samples were also investigated using COMSOL Multiphysics. This study employed the Dielectric Material Test Fixture, for the first time, to measure the permittivity of foam samples thanks to our 3D-printed holder. The SEM images confirmed that the CNTs established interconnected and evenly distributed networks on the PU surface of all CNT-PU samples. The AC conductivity increased with increasing frequency and CNT content, and the highest value of 0.0068 S/cm was recorded for 11.2 wt.% CNT sample at 10 MHz. Additionally, the permittivity (real and imaginary parts) of our samples increased with increasing CNT content but decreased with increasing frequency. At 1000 MHz, the complex permittivity increased from 1.32 – j 0.0059 for PU foam to 8.65 – j 3.70 for 11.2 wt.% CNT sample. Similarly, the same sample recorded the highest complex permittivity value of 3.76 – j 3.56 at 25 GHz. The total shielding effectiveness was significantly improved by the conductive networks, confirmed by SEM images, located on the PU surfaces. Two of our prepared samples (6 wt.% CNT and 11.2 wt.% CNT) fulfilled the standard commercial requirements for EMI shielding applications in the 18 – 26.5 GHz frequency range. The total shielding effectiveness was also greatly enhanced with the increment of CNT amount. The intensity of the electric field passing through the samples significantly dropped with increasing the CNT filler concentration. The prepared samples exhibited a strong absorption performance in dissipating EM energy; such a feature is very advantageous and preferred in the EMI shielding industry because it reduces the EMI in the environment. This study could be performed using different foam matrices with higher values of permittivity. Different conductive fillers could also be used to enhance the dielectric properties of shielding materials.

Declarations

Author contributions:

Ahmad Khamis: Writing – review & editing, Writing – original draft, Data curation, Investigation, Formal analysis. Laetitia Urbanczyk: Conceptualization, Methodology, Investigation, Writing - review & editing. Christophe Detrembleur: Project administration, Methodology, Resources, Writing – review & editing, Supervision, Funding acquisition. Isabelle Huynen: Writing – review & editing, Writing – original draft, Formal analysis, Project administration; Resources, Supervision, Funding acquisition. All authors approved the final version of this article.

Funding: This work was performed in the frame of the UP_Plastics project co-funded by the European Union and the Walloon Region as part of the FEDER 2021-2027 Program.

Data availability: The data that support the findings of this study are available upon reasonable request.

Acknowledgments: The authors thank Pascal Simon and Benoît Hubert from the Welcome technological platform of UCLouvain for their great support in the measurements of CNT-PU samples. Benoît Hubert designed and fabricated the 3D-printed holder for the DMTF. The works of I. Huynen and C. Detrembleur as research directors are funded by the National Fund for Scientific Research (FNRS, Belgium).

Competing interests: The authors have no relevant financial or non-financial interests to disclose.

References

[1] S. Meena, N. Kumari, V. Gahlaut, C. Shekhar, S. Mitra, and U. K. Dwivedi, "Electrical and EMI shielding studies of ferrite/MWCNTs/PVDF composites," *Journal of Applied Polymer Science*, pp. e56446.

[2] H. Kim, S. Jeon, Y. S. Cho, C. Huang, S. Na, J. Lee, Y. Chung, J. Kang, S. W. Kim, and D. Choi, "Polydopamine-coated iron-nickel alloy and epoxy composites for electromagnetic interference shielding," *Journal of Applied Polymer Science,* vol. 141, no. 44, pp. e56187, 2024.

[3] M. Magioli, B. Soares, A. Sirqueira, M. Rahaman, and D. Khastgir, "EMI shielding effectiveness and dielectrical properties of SBS/PAni. DBSA blends: Effect of blend preparation," *Journal of applied polymer science,* vol. 125, no. 2, pp. 1476-1485, 2012.

[4] R. Hsissou, R. Seghiri, Z. Benzekri, M. Hilali, M. Rafik, and A. Elharfi, "Polymer composite materials: A comprehensive review," *Composite structures,* vol. 262, pp. 113640, 2021.

[5] R. K. Mishra, M. G. Thomas, J. Abraham, K. Joseph, and S. Thomas, "Electromagnetic interference shielding materials for aerospace application: A state of the art," *Advanced materials for electromagnetic shielding: fundamentals, properties, and applications*, pp. 327-365, 2018.

[6] M. H. Al-Saleh, and U. Sundararaj, "Electromagnetic interference shielding mechanisms of CNT/polymer composites," *Carbon,* vol. 47, no. 7, pp. 1738-1746, 2009.

[7] M. G. Jang, S. C. Ryu, K. J. Juhn, S. K. Kim, and W. N. Kim, "Effects of carbon fiber modification with multiwall CNT on the electrical conductivity and EMI shielding effectiveness of polycarbonate/carbon fiber/CNT composites," *Journal of applied polymer science,* vol. 136, no. 14, pp. 47302, 2019.

[8] L. Guohua, Z. Zhiyong, and W. Yangang, "Research progress on highly conductive polymer composites based on carbon-based nanofillers," *Polymer Composites*, 2025.

[9] S. Bayda, M. Adeel, T. Tuccinardi, M. Cordani, and F. Rizzolio, "The history of nanoscience and nanotechnology: from chemical–physical applications to nanomedicine," *Molecules,* vol. 25, no. 1, pp. 112, 2019.

[10] X. Cheng, "Nanostructures: fabrication and applications," *Nanolithography*, pp. 348-375: Elsevier, 2014.

[11] S. Malik, K. Muhammad, and Y. Waheed, "Nanotechnology: a revolution in modern industry," *Molecules,* vol. 28, no. 2, pp. 661, 2023.

[12] S. Alfei, and G. Zuccari, "Last Fifteen Years of Nanotechnology Application with Our Contribute," *Nanomaterials,* vol. 15, no. 4, pp. 265, 2025.

[13] S. A. Zaidi, and J. H. Shin, "Recent developments in nanostructure based electrochemical glucose sensors," *Talanta,* vol. 149, pp. 30-42, 2016.

[14] N. Chikyu, T. Nakano, G. Kletetschka, and Y. Inoue, "Excellent electromagnetic interference shielding characteristics of a unidirectionally oriented thin multiwalled carbon nanotube/polyethylene film," *Materials & Design,* vol. 195, pp. 108918, 2020.

[15] V. S. Eswaraiah, Venkataraman; Ramaprabhu, Sundara, "Functionalized graphene–PVDF foam composites for EMI shielding," *Macromolecular Materials and Engineering,* vol. 296, no. 10, pp. 894-898, 2011.

[16] S. Chen, K. Li, G. Wang, W. Ding, X. Zhang, Y. Zhao, Y. Yang, and J. Chen, "Microcellular foamed bilayer iPP/CNTs-HDPE/CNTs nanocomposites for electromagnetic interference shielding application," *Journal of Polymer Research,* vol. 31, no. 12, pp. 357, 2024.

[17] S. Sultana, M. Rahaman, and M. R. Chandan, "Enhancing EMI Shielding Efficiency of Polyurethane Foam by Incorporating MWCNT-Decorated Hollow Glass Microspheres," *ACS omega*, 2025.

[18] C. K. Kum, Y.-T. Sung, M. S. Han, W. N. Kim, H. S. Lee, S.-J. Lee, and J. Joo, "Effects of morphology on the electrical and mechanical properties of the polycarbonate/multi-walled carbon nanotube composites," *Macromolecular Research,* vol. 14, pp. 456-460, 2006.

[19] J.-M. Thomassin, C. Pagnoulle, L. Bednarz, I. Huynen, R. Jerome, and C. Detrembleur, "Foams of polycaprolactone/MWNT nanocomposites for efficient EMI reduction," *Journal of Materials Chemistry,* vol. 18, no. 7, pp. 792-796, 2008.

[20] K. Chizari, M. Arjmand, Z. Liu, U. Sundararaj, and D. Therriault, "Three-dimensional printing of highly conductive polymer nanocomposites for EMI shielding applications," *Materials Today Communications,* vol. 11, pp. 112-118, 2017.

[21] S. Sultana, and M. R. Chandan, "Enhanced EMI Shielding Efficiency of Graphene Nanoplatelets and Glass Sphere Composite-Loaded Ultralight Weight Flexible Polyurethane Foam," *Polymers for Advanced Technologies,* vol. 35, no. 10, pp. e6611, 2024.

[22] S. Jafarzadeh, A. Farzaneh, V. Haddadi-Asl, and I. S. Jouibari, "A review on electrically conductive polyurethane nanocomposites: From principle to application," *Polymer Composites,* vol. 44, no. 12, pp. 8266-8302, 2023.

[23] Z. E. Zadeh, A. Solouk, M. Shafieian, and M. H. Nazarpak, "Electrospun polyurethane/carbon nanotube composites with different amounts of carbon nanotubes and almost the same fiber diameter for biomedical applications," *Materials Science and Engineering: C,* vol. 118, pp. 111403, 2021.

[24] K. Nakagawa, "Foam materials made from carbon nanotubes," *Carbon Nanotubes-From Research to Applications*, 2011.

[25] Q. Xu, and W. Zhang, "Improvement of the electromechanical properties of thermoplastic polyurethane composite by ionic liquid modified multiwall carbon nanotubes," *e-Polymers,* vol. 21, no. 1, pp. 166-178, 2021.

[26] D. Zhang, H. Yang, J. Pan, B. Lewis, W. Zhou, K. Cai, A. Benatar, L. J. Lee, and J. M. Castro, "Multi-functional CNT nanopaper polyurethane nanocomposite fabricated by ultrasonic infiltration and dip soaking processes," *Composites Part B: Engineering,* vol. 182, pp. 107646, 2020.

[27] X. Huang, D. Yu, and S. Wang, "Microwave Absorption Properties of Multi-Walled Carbon Nanotubes/Carbonyl Iron Particles/Polyurethane Foams," *Materials,* vol. 15, no. 16, pp. 5690, 2022.

[28] E. Zawadzak, M. Bil, J. Ryszkowska, S. N. Nazhat, J. Cho, O. Bretcanu, J. A. Roether, and A. R. Boccaccini, "Polyurethane foams electrophoretically coated with carbon nanotubes for tissue engineering scaffolds," *Biomedical Materials,* vol. 4, no. 1, pp. 015008, 2008.

[29] X. Wang, H. Li, T. Wang, X. Niu, Y. Wang, S. Xu, Y. Jiang, L. Chen, and H. Liu, "Flexible and high-performance piezoresistive strain sensors based on multi-walled carbon nanotubes@ polyurethane foam," *RSC advances,* vol. 12, no. 22, pp. 14190-14196, 2022.

[30] X.-C. Zhang, F. Scarpa, R. McHale, A. P. Limmack, and H.-X. Peng, "Carbon nano-ink coated open cell polyurethane foam with micro-architectured multilayer skeleton for damping applications," *RSC Advances,* vol. 6, no. 83, pp. 80334-80341, 2016.

[31] A. Tewari, S. Gandla, S. Bohm, C. R. McNeill, and D. Gupta, "Highly exfoliated MWNT–rGO ink-wrapped polyurethane foam for piezoresistive pressure sensor applications," *ACS applied materials & interfaces,* vol. 10, no. 6, pp. 5185-5195, 2018.

[32] M. Nabeel, M. Mousa, B. Viskolcz, B. Fiser, and L. Vanyorek, "Recent advances in flexible foam pressure sensors: manufacturing, characterization, and applications–a review," *Polymer Reviews,* vol. 64, no. 2, pp. 449-489, 2024.

[33] H. Xu, Y. Zhang, and F. Zheng, "Study on measuring method of dielectric spectroscopy for polymer dielectrics," in 2009 IEEE 9th International Conference on the Properties and Applications of Dielectric Materials, 2009, pp. 922-925.

[34] A. Hosseinbeig, S. Marathe, and D. Pommerenke, "Characterization of relative complex permittivity and permeability for magneto-dielectric sheets," *IEEE Transactions on Electromagnetic Compatibility,* vol. 60, no. 6, pp. 1786-1794, 2017.

[35] S. Hang, and W. Xue-tao, "Application of COMSOL multiphysics in thermal effect analysis of electromagnetic active vibration absorber," in IOP Conference Series: Materials Science and Engineering, 2017, pp. 012037.

[36] A. Akdagli, and K. Guney, "New wide-aperture-dimension formula obtained by using a particle swarm optimization for optimum gain pyramidal horns," *Microwave and Optical Technology Letters,* vol. 48, no. 6, pp. 1201-1205, 2006.

[37] H.-Z. Ma, J.-N. Zhao, R. Tang, Y. Shao, K. Ke, K. Zhang, B. Yin, and M.-B. Yang, "Polypyrrole@ CNT@ PU Conductive Sponge-Based Triboelectric Nanogenerators for Human Motion Monitoring and Self-Powered Ammonia Sensing," *ACS Applied Materials & Interfaces,* vol. 15, no. 47, pp. 54986-54995, 2023.

[38] D. Wu, M. Wei, R. Li, T. Xiao, S. Gong, Z. Xiao, Z. Zhu, and Z. Li, "A percolation network model to predict the electrical property of flexible CNT/PDMS composite films fabricated by spin coating technique," *Composites Part B: Engineering,* vol. 174, pp. 107034, 2019.

[39] P. R. Connolly, M. Josh, K. T. O'Neill, S. J. Seltzer, M. O. Wigand, M. B. Clennell, E. F. May, and M. L. Johns, "Dielectric polarization studies in partially saturated shale cores," *Journal of Geophysical Research: Solid Earth,* vol. 124, no. 11, pp. 10721-10734, 2019.

[40] A. S. Hoang, "Electrical conductivity and electromagnetic interference shielding characteristics of multiwalled carbon nanotube filled polyurethane composite films," *Advances in Natural Sciences: Nanoscience and Nanotechnology,* vol. 2, no. 2, pp. 025007, 2011.

[41] I. V. Novikov, D. V. Krasnikov, A. M. Vorobei, Y. I. Zuev, H. A. Butt, F. S. Fedorov, S. A. Gusev, A. A. Safonov, E. V. Shulga, and S. D. Konev, "Multifunctional elastic nanocomposites with extremely low concentrations of single-walled carbon nanotubes," *ACS Applied Materials & Interfaces,* vol. 14, no. 16, pp. 18866-18876, 2022.

[42] M. Yanılmaz, and A. S. Sarac, "A review: effect of conductive polymers on the conductivities of electrospun mats," *Textile Research Journal,* vol. 84, no. 12, pp. 1325-1342, 2014.

[43] S. Bronnikov, S. Kostromin, M. Asandulesa, D. Pankin, and A. Podshivalov, "Interfacial interactions and interfacial polarization in polyazomethine/MWCNTs nanocomposites," *Composites Science and Technology,* vol. 190, pp. 108049, 2020.

[44] T. Durance, and P. Yaghmaee, "4.51-microwave dehydration of food and food ingredients," *Comprehensive biotechnology*, pp. 617-628, 2011.

[45] J. Wu, Y. Gao, W. Hu, and Z. Lu, "Influence of carbon nanotubes on the absorption performance and mechanical behavior of basalt fiber composite materials," *Polymer Composites,* vol. 46, no. 4, pp. 3109-3121, 2025.

[46] B. Wang, Y. Liu, M. Dong, and G. Zuo, "Study on changing the dielectric constant and radar reflection of foamed polyurethane by adding graphite," in Journal of Physics: Conference Series, 2021, pp. 012004.

[47] K. Shehzad, Z.-M. Dang, M. N. Ahmad, R. U. R. Sagar, S. Butt, M. U. Farooq, and T.-B. Wang, "Effects of carbon nanotubes aspect ratio on the qualitative and quantitative aspects of frequency response of electrical conductivity and dielectric permittivity in the carbon nanotube/polymer composites," *Carbon,* vol. 54, pp. 105-112, 2013.

[48] M. C. Sekhar, P. Kondaiah, S. J. Chandra, G. M. Rao, and S. Uthanna, "Effect of substrate bias voltage on the structure, electric and dielectric properties of TiO2 thin films by DC magnetron sputtering," *Applied Surface Science,* vol. 258, no. 5, pp. 1789-1796, 2011.

[49] B. Huang, J. Yue, B. Fan, Y. Liu, and X. Huang, "Vertical carbon nanotubes arrays with controlled morphology on silicon carbide fibers for electromagnetic wave absorption," *Ceramics International,* vol. 48, no. 13, pp. 19375-19381, 2022.

[50] M. Qin, L. Zhang, and H. Wu, "Dielectric loss mechanism in electromagnetic wave absorbing materials," *Advanced Science,* vol. 9, no. 10, pp. 2105553, 2022.
[51] S. P. Walch, "The bonding of NOz, NH, and CHI" to models of a (10, O) carbon nanotube."
[52] A. Mora, P. Verma, and S. Kumar, "Electrical conductivity of CNT/polymer composites: 3D printing, measurements and modeling," *Composites Part B: Engineering,* vol. 183, pp. 107600, 2020.
[53] F. Caspers, "RF engineering basic concepts: S-parameters," *arXiv preprint arXiv:1201.2346*, 2012.
[54] Y. Luo, Y. Guo, C. Wei, J. Chen, G. Zhao, Q. Yuan, and Y. Zhu, "Lightweight, compressible, and stretchable composite foams for ultra-efficient and high-stable electromagnetic interference shielding materials," *Carbon,* vol. 215, pp. 118480, 2023.
[55] R. R Mohan, S. J. Varma, and J. Sankaran, "Impressive electromagnetic shielding effects exhibited by highly ordered, micrometer thick polyaniline films," *Applied Physics Letters,* vol. 108, no. 15, 2016.
[56] M. H. Al-Saleh, G. A. Gelves, and U. Sundararaj, "Copper nanowire/polystyrene nanocomposites: Lower percolation threshold and higher EMI shielding," *Composites Part A: Applied Science and Manufacturing,* vol. 42, no. 1, pp. 92-97, 2011.
[57] K. Huang, M. Chen, G. He, X. Hu, W. He, X. Zhou, Y. Huang, and Z. Liu, "Stretchable microwave absorbing and electromagnetic interference shielding foam with hierarchical buckling induced by solvent swelling," *Carbon,* vol. 157, pp. 466-477, 2020.
[58] G. Sang, P. Xu, T. Yan, V. Murugadoss, N. Naik, Y. Ding, and Z. Guo, "Interface engineered microcellular magnetic conductive polyurethane nanocomposite foams for electromagnetic interference shielding," *Nano-Micro Letters,* vol. 13, no. 1, pp. 153, 2021.
[59] Z. Lei, D. Tian, X. Liu, J. Wei, K. Rajavel, T. Zhao, Y. Hu, P. Zhu, R. Sun, and C.-P. Wong, "Electrically conductive gradient structure design of thermoplastic polyurethane composite foams for efficient electromagnetic interference shielding and ultra-low microwave reflectivity," *Chemical Engineering Journal,* vol. 424, pp. 130365, 2021.
[60] K. Sushmita, A. V. Menon, S. Sharma, A. C. Abhyankar, G. Madras, and S. Bose, "Mechanistic insight into the nature of dopants in graphene derivatives influencing electromagnetic interference shielding properties in hybrid polymer nanocomposites," *The Journal of Physical Chemistry C,* vol. 123, no. 4, pp. 2579-2590, 2019.
[61] S. P. Pawar, and S. Bose, "Extraordinary synergy in attenuating microwave radiation with cobalt-decorated graphene oxide and carbon nanotubes in polycarbonate/poly (styrene-co-acrylonitrile) blends," *ChemNanoMat,* vol. 1, no. 8, pp. 603-614, 2015.
[62] Y. Zhao, J. Hou, Z. Bai, Y. Yang, X. Guo, H. Cheng, Z. Zhao, X. Zhang, J. Chen, and C. Shen, "Facile preparation of lightweight PE/PVDF/Fe3O4/CNTs nanocomposite foams with high conductivity for efficient electromagnetic interference shielding," *Composites Part A: Applied Science and Manufacturing,* vol. 139, pp. 106095, 2020.